

Molecular classification to refine surgical and radiotherapeutic decision-making in meningioma

Received: 16 December 2023

Accepted: 1 July 2024

Published online: 21 August 2024

 Check for updates

A list of authors and their affiliations appears at the end of the paper

Treatment of the tumor and dural margin with surgery and sometimes radiation are cornerstones of therapy for meningioma. Molecular classifications have provided insights into the biology of disease; however, response to treatment remains heterogeneous. In this study, we used retrospective data on 2,824 meningiomas, including molecular data on 1,686 tumors and 100 prospective meningiomas, from the RTOG-0539 phase 2 trial to define molecular biomarkers of treatment response. Using propensity score matching, we found that gross tumor resection was associated with longer progression-free survival (PFS) across all molecular groups and longer overall survival in proliferative meningiomas. Dural margin treatment (Simpson grade 1/2) prolonged PFS compared to no treatment (Simpson grade 3). Molecular group classification predicted response to radiotherapy, including in the RTOG-0539 cohort. We subsequently developed a molecular model to predict response to radiotherapy that discriminates outcome better than standard-of-care classification. This study highlights the potential for molecular profiling to refine surgical and radiotherapy decision-making.

Meningiomas are the most common primary intracranial tumor in adults^{1,2}. Maximal resection of both the meningioma and its dural attachments has historically been the primary goal of surgery, with Simpson grade used as a metric to define extent of resection (EOR)^{3–8}. However, contemporary studies have challenged the universal benefit of aggressive surgical strategies, including dural resection in every case, particularly if it places critical neurovascular structures at risk^{7–9}. Aside from surgery, radiotherapy (RT) remains the sole alternative treatment for these tumors, generally reserved as adjuvant therapy for aggressive, recurrent or incompletely resected meningiomas^{10–20}. However, rates of tumor control after adjuvant RT are highly variable, creating a need to determine better predictors of response^{17,21,22}.

Although several new molecular classifications and prognostic systems have been described for meningiomas, response to surgery and RT continues to vary considerably among patients, and the role of treatment in the context of these molecular biomarkers has not been fully explored^{23–30}. Furthermore, although ongoing randomized trials are examining the efficacy of RT in a subset of patients with

meningioma, molecular features were not used for treatment stratification, as most were discovered after the inception of these studies^{31,32}.

To address these critical gaps, a large cohort of clinically annotated, molecularly profiled meningiomas, including invaluable data from a prospective clinical trial (NRG Oncology RTOG-0539; [NCT00895622](https://clinicaltrials.gov/ct2/show/study/NCT00895622)), were used in propensity score matching (PSM) to (1) determine the benefit of EOR and additive dural treatment (Simpson grade) in the context of molecular biomarkers; (2) determine the capability of molecular classification to predict response to RT; and (3) create and validate molecular predictive models of response to RT using prospective clinical trial samples that are made publicly available to help inform RT treatment decisions^{17,22,33}.

Results

Clinical and molecular cohort

A total of 2,824 retrospective meningiomas were assembled, of which 1,686 tumors from 10 institutions had molecular and clinical outcomes data (Extended Data Fig. 1, Extended Data Table 1 and

✉ e-mail: farshad.nassiri@uhn.ca; gelareh.zadeh@uhn.ca

Supplementary Table 1). Subsets of this cohort were used for specific analyses for EOR, Simpson grade and RT, respectively (Fig. 1a,b), including a separate, prospectively collected cohort of 100 meningiomas from the NRG Oncology RTOG-0539 phase 2 clinical trial used for both validation of findings from the retrospective RT analysis and for independent biomarker discovery and predictive modeling (Table 1 and Extended Data Table 2). Given the key differences in baseline covariates between the different treatment arms compared throughout the study (for example, in comparing gross total resection (GTR) versus subtotal resection (STR), there were more recurrent meningiomas, meningiomas in skull base locations and tumors that received adjuvant RT in the latter group compared to the former), PSM was performed to balance these covariates in a systematic and standardized manner for our analyses of GTR versus STR, Simpson grades 1/2 versus 3, Simpson grade 1 versus grade 2 and receipt of adjuvant RT versus observation.

All meningiomas in our study with DNA methylation data were first classified using the DKFZ Central Nervous System tumor classifier v.12.5 (<https://www.molecularneuropathology.org/>) to confirm the molecular diagnosis of meningioma before being stratified into other meningioma molecular classification and prognostic systems (Fig. 1c,d and Extended Data Fig. 2)^{24–29,34}. Primary analyses used the Toronto Molecular Groups (henceafter referred to as just ‘Molecular Groups’ in the manuscript) as it performed optimally for outcome prediction (Extended Data Fig. 2b and Extended Data Table 1), whereas sensitivity analyses were performed and detailed for other molecular classification and prognostic systems. Overall, Hypermetabolic and Proliferative meningiomas had a higher burden of copy number variants (CNVs), including losses of chromosomes 1p, 10, 14, 18 and 22q, compared to Immunogenic and NF2-wild-type (NF2-wt) meningiomas irrespective of institution (Extended Data Fig. 1). In keeping with previous work, progression-free survival (PFS) outcomes declined in a stepwise manner from Immunogenic to NF2-wt to Hypermetabolic to Proliferative meningiomas, respectively, with overall survival (OS) following a similar trend (Fig. 1f,h)^{24,27}.

Impact of surgical resection across Molecular Groups

Although EOR is known to be important for meningiomas, its benefit in the context of molecular classification is unclear. A significant interaction was found between EOR and Molecular Group ($P = 0.018$ and $P = 0.035$ for PFS and OS, respectively). GTR appeared to confer a significant PFS benefit for meningiomas in all Molecular Groups (Extended Data Fig. 3a–d). When controlling for World Health Organization (WHO) grade, primary/recurrent tumor status and receipt of adjuvant RT, local tumor control after GTR was significantly less durable for Hypermetabolic (STR:GTR hazard ratio (HR) = 1.77, 95% confidence interval (CI): 1.28–2.43, $P = 4.7 \times 10^{-4}$) and Proliferative meningiomas (HR = 1.58, 95% CI: 1.14–2.22, $P = 0.013$) than for Immunogenic and NF2-wt tumors (Extended Data Fig. 3e). When OS outcomes were similarly examined across Molecular Groups, STR was primarily associated with significantly worse OS in Proliferative meningiomas (HR = 1.90, 95% CI: 1.28–2.82, $P = 0.002$), but not in meningiomas from other Molecular Groups (Extended Data Fig. 3f–j). However, when all cases were considered in multivariable analyses, regardless of the molecular classification or prognostic system used to risk stratify these tumors, including when prognostic CNVs were considered, GTR was consistently associated with improved PFS and OS compared to STR (Extended Data Fig. 4 and Supplementary Figs. 2 and 3). Results were concordant when only recurrent meningiomas were considered (Supplementary Fig. 4). This suggests that, regardless of tumor biology, complete surgical resection remains the critical determinant of local control, even in the recurrent setting, but its benefits may be attenuated in the most biologically aggressive meningiomas.

To examine the relationship between EOR and Molecular Group in more granular detail while further controlling for baseline covariate differences, PSM was performed for age, sex, WHO grade,

primary/recurrent tumor status, receipt of adjuvant RT, tumor location and Molecular Group between the GTR and STR groups (Fig. 2a–f and Supplementary Tables 2 and 3). After PSM, STR remained significantly associated with worse PFS (HR = 2.02, 95% CI: 1.49–2.73, $P = 5.2 \times 10^{-6}$; Fig. 2e,f). This finding remained consistent when analyses were repeated using other molecular classification and prognostic systems (Extended Data Fig. 5 and Supplementary Tables 4–9), including when sensitivity analyses were performed using multiple imputation and PSM to address missing data (Supplementary Tables 10–23).

Impact of treating dural margins

A benchmark for meningioma surgery historically has been aggressive resection of the tumor’s dural margins in addition to the tumor itself, with the view that this will further reduce recurrence risk. In instances where aggressive excision of these dural elements may not be safe or feasible (Simpson grade 1), they can be either thermocoagulated (Simpson grade 2) or left in situ (Simpson grade 3). To first determine the impact of any type of dural margin treatment, meningiomas that received either a Simpson grade 1 or 2 resection were grouped together. These meningiomas had significantly improved PFS compared to tumors that were completely macroscopically removed without any adjunctive dural excision or coagulation (Simpson grade 3; Fig. 2b,g). Conversely, among meningiomas with dural treatment (Simpson grades 1 or 2), there was no significant PFS difference between tumors that received complete dural margin excision (Simpson grade 1) versus those with dural margins treated with thermocoagulation alone (Simpson grade 2; Fig. 2b,k).

After PSM, meningiomas that received a Simpson grade 3 resection still had significantly shorter time to recurrence compared to those that received a Simpson grade 1/2 resection (HR = 1.64, 95% CI: 1.03–2.62, $P = 0.038$; Fig. 2h–j and Supplementary Table 24). Additionally, achieving a Simpson grade 1 resection still did not confer a significant PFS benefit compared to a Simpson grade 2 resection after PSM (HR = 0.87, 95% CI: 0.52–1.44, $P = 0.58$; Fig. 2l–n). These findings were consistent across other molecular classification and prognostic systems (Extended Data Fig. 5 and Supplementary Tables 4–9) and again even with PSM after multiple imputation (Supplementary Tables 10–23).

On multivariable analysis, like EOR, there was a significant interaction between Simpson grade and Molecular Group ($P = 0.049$). After controlling for age, sex, WHO grade, tumor location and receipt of adjuvant RT, obtaining a GTR without any dural treatment (Simpson grade 3) was associated with worse PFS in NF2-wt (HR = 3.32, 95% CI: 1.42–7.74, $P = 0.005$) and Immunogenic meningiomas (HR = 5.88, 95% CI: 0.96–36.16, $P = 0.056$; Extended Data Fig. 6a,c) compared to Hypermetabolic and Proliferative tumors; however, there was no significant PFS benefit for specifically obtaining a Simpson grade 1 resection versus a Simpson grade 2 resection for meningiomas in any Molecular Group (Extended Data Fig. 6b,d).

Overall, these findings suggest that while there is clear additive benefit to treating the dural margins in addition to complete tumor resection, pursuing aggressive dural excision in every case may not appreciably improve oncologic outcomes compared to just thermocoagulation of these attachments alone.

Defining a group of RT-resistant meningiomas

Adjuvant RT is currently the only adjunctive standard-of-care treatment aside from surgery for meningiomas and is generally selected for ‘high-risk’ patients based on WHO grade and/or the presence of residual tumor after surgery. However, response to RT in meningiomas is highly variable, and contemporary clinical practice reflects this uncertainty by including RT as a treatment option for meningiomas across all WHO grades.

To look at this more specifically, all meningiomas in the retrospective cohort were first examined. Some of the heterogeneity in overall outcomes were found to be resolved by Molecular Group

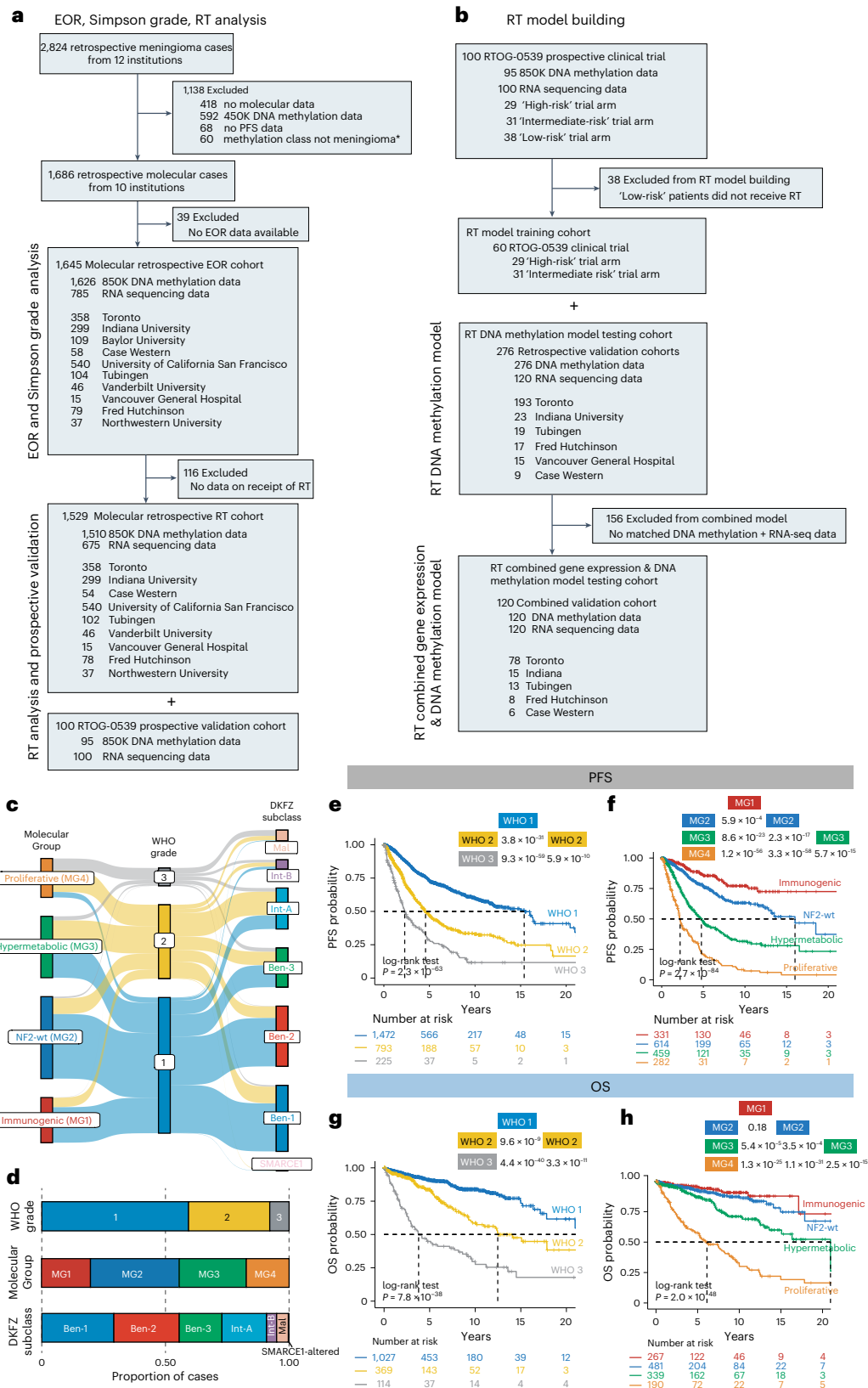


Fig. 1 | Meningioma cohort stratified based on molecular classification and the role of EOR. a, b, CONSORT diagram demonstrating the cohort of meningiomas used in this study, the sequence of analyses and results presented and the respective institutions from where these samples were obtained for our EOR, Simpson grade, and RT analyses (a) and for RT model building (b). **c, d,** Sankey plot (c) and bar plots (d) showing the relationship of WHO grading with molecular classifications (Molecular Group (MG) for primary analysis and

DKFZ methylation subclass to confirm the molecular diagnosis of meningioma). **e, f,** Kaplan–Meier survival curves showing PFS of meningiomas based on WHO grade (e) and MG (f). **g–h,** OS of meningiomas used in our study based on classification by WHO grade (g) and MG (h). Inset shows the *P* values from the pairwise log-rank test between groups with Benjamini–Hochberg correction for multiple comparisons.

Table 1 | Baseline characteristics of the retrospective meningioma cohort with EOR, stratified by EOR

Baseline characteristic	Total EOR cohort	GTR (n=1,458)	STR (n=696)	P value
Median age (IQR)	57 (47–67)	58 (47–67)	57 (47–67)	0.667
Biological sex				
Male	714	486 (33%)	228 (33%)	0.829
Female	1,385	934 (64%)	451 (65%)	0.775
Tumor status (at index surgery)				
Primary	1,371	955 (66%)	416 (60%)	1.11 × 10⁻³
Recurrent	317	161 (11%)	156 (22%)	5.14 × 10⁻¹²
WHO grade				
1	1,317	907 (62%)	410 (59%)	0.154
2	638	425 (29%)	213 (31%)	0.522
3	199	126 (9%)	73 (10%)	0.192
Molecular Group (MG)				
1 (Immunogenic)	322	243 (17%)	79 (11%)	1.52 × 10⁻³
2 (NF2-wild-type)	588	418 (29%)	170 (24%)	4.38 × 10⁻²
3 (Hypermetabolic)	453	298 (20%)	155 (22%)	0.358
4 (Proliferative)	282	174 (12%)	108 (16%)	2.53 × 10⁻²
Methylation subclass (DKFZ)				
Benign, subclass 1 (Ben-1)	477	342 (23%)	135 (19%)	3.87 × 10⁻²
Benign, subclass 2 (Ben-2)	428	315 (22%)	113 (16%)	4.20 × 10⁻³
Benign, subclass 3 (Ben-3)	278	179 (13%)	99 (14%)	0.233
Intermediate, subclass A (Int-A)	293	191 (13%)	102 (15%)	0.359
Intermediate, subclass B (Int-B)	64	40 (3%)	24 (4%)	0.444
Malignant (Mal)	80	53 (4%)	27 (4%)	0.874
SMARCE1-altered	6	6 (0%)	0	0.209
Simpson grade				
1	338	338 (24%)	0	2.20 × 10⁻¹⁶
2	382	382 (27%)	0	2.20 × 10⁻¹⁶
3	166	166 (11%)	0	2.20 × 10⁻¹⁶
4	696	0	696 (100%)	2.20 × 10⁻¹⁶
Adjuvant RT				
Yes	382	186 (15%)	196 (29%)	3.53 × 10⁻¹⁸
No	1,527	1,069 (72%)	458 (65%)	4.00 × 10⁻⁵
Location				
Supratentorial non-skull base (ST-non-SB)	599	442 (29%)	157 (22%)	1.34 × 10⁻³
Supratentorial skull base (ST-SB)	405	241 (16%)	164 (23%)	2.18 × 10⁻⁵
Infratentorial non-skull base (IT-non-SB)	39	21 (1%)	18 (3%)	6.98 × 10⁻²
Infratentorial skull base (IT-SB)	206	106 (7%)	100 (14%)	5.11 × 10⁻⁸
Other	33	29 (4%)	4 (1%)	2.60 × 10⁻²
Median PFS (95% CI)		12.2 (10.7–16.4)	4.5 (3.9–4.9)	1.87 × 10⁻²⁶
Median OS (95% CI)		17.8 (15.2–NA) [†]	14.9 (13.0–NA) [†]	3.23 × 10⁻⁴

IQR, interquartile range. [†]Upper limit of 95% CI not met. P values were obtained from Fisher's exact test (two-tailed) for categorical variables and unpaired Welch's two-sample t-test for continuous variables (two-tailed). Bolded P values in the table indicate $P < 0.05$.

classification, even for cases within each WHO grade (Fig. 3a–h). When the retrospective cohort was then stratified based on EOR (GTR versus STR) and receipt of adjuvant RT (RT versus observation), adjuvant RT significantly prolonged PFS after STR for Immunogenic meningiomas ($P = 0.036$) and moderately for NF2-wt meningiomas ($P = 0.14$) (Fig. 3i,j). For Hypermetabolic meningiomas, only marginal improvement of PFS was observed when RT was added to either GTR ($P = 0.950$) or STR ($P = 0.136$) (Fig. 3k) cases on Kaplan–Meier analysis. Proliferative meningiomas, however, had almost universally short PFS regardless of treatment paradigm, although tumors that received both GTR and adjuvant RT appeared to have incrementally better outcomes (Fig. 3l).

In the retrospective cohort, the meningiomas treated with adjuvant RT after surgery had similar PFS outcomes across Molecular Groups as in the complete cohort that included cases without RT (Fig. 4a). However, there were also significant baseline differences between the RT-treated meningiomas compared to those that were observed after surgery without RT, reflecting the real-world biases of preferentially irradiating higher WHO grade, recurrent and STR cases (Supplementary Table 25). PSM was again performed to control for these specific covariates (which were the same as those used for risk stratification in the RTOG-0539 clinical trial) between the RT and observation (Obs) arms in the retrospective cohort (Fig. 4b,c). Following this and stratification of matched cases into individual Molecular Groups, adjuvant RT was now associated with significantly prolonged PFS in molecularly defined Immunogenic, NF2-wt and Hypermetabolic meningiomas but not in Proliferative meningiomas (Fig. 4c). When this analysis was repeated in only incompletely resected (STR) meningiomas—a challenging cohort to manage clinically ($n = 512$; Supplementary Fig. 5 and Supplementary Table 26)—the significant benefit of adjuvant RT was retained in STR Immunogenic and NF2-wt meningiomas (Supplementary Fig. 5c,d) with a signal toward longer PFS in Hypermetabolic tumors although not reaching statistical significance in this group ($P = 0.150$; Supplementary Fig. 5e). STR Proliferative meningiomas clearly still did not benefit from adjuvant RT ($P = 0.20$; Supplementary Fig. 5f).

To validate these findings using the NRG Oncology RTOG-0539 cohort, DNA methylation ($n = 95$) and RNA sequencing (RNA-seq) ($n = 100$) data were generated on these meningioma samples, and they were stratified into the four Molecular Groups in the same manner as the retrospective cohort (Fig. 4d–f and Extended Data Table 2). Outcomes of meningiomas in the prospective RTOG-0539 cohort that received surgery and adjuvant RT resembled those of the retrospective meningioma cohort, notably with Hypermetabolic and Proliferative meningiomas accounting for nearly all progressive tumors in the trial (Fig. 4g). To further validate our findings above, the prospective RTOG-0539 cases that received adjuvant RT were treated as an 'RT' arm, and PSM was performed for WHO grade, EOR, primary/recurrent tumor status and Molecular Group, with cases from our retrospective cohort of meningiomas that did not receive RT as the 'observation' arm to simulate 'randomization' (Fig. 4h,i). After this PSM, adjuvant RT was still significantly associated with prolonged PFS in Immunogenic, NF2-wt and Hypermetabolic meningiomas compared to observation alone but not in Proliferative meningiomas (Fig. 4j), validating that Proliferative meningiomas may be largely RT resistant. In the context of these findings, if the risk stratification of the original RTOG-0539 risk groups is re-examined, 23 of 58 (40%) cases that received adjuvant RT ('intermediate-risk' and 'high-risk') could be classified as RT-resistant Proliferative meningiomas, whereas 35 of 36 (97%) of the 'low-risk' (observation) group were non-Proliferative tumors that could be deemed RT responsive (Fig. 4e). This is particularly important as RT-resistant Proliferative meningiomas can be found across all WHO grades (Fig. 3c–e), providing further rationale for future molecularly informed clinical trials that may be able to triage these RT-resistant meningiomas to systemic/experimental therapies.

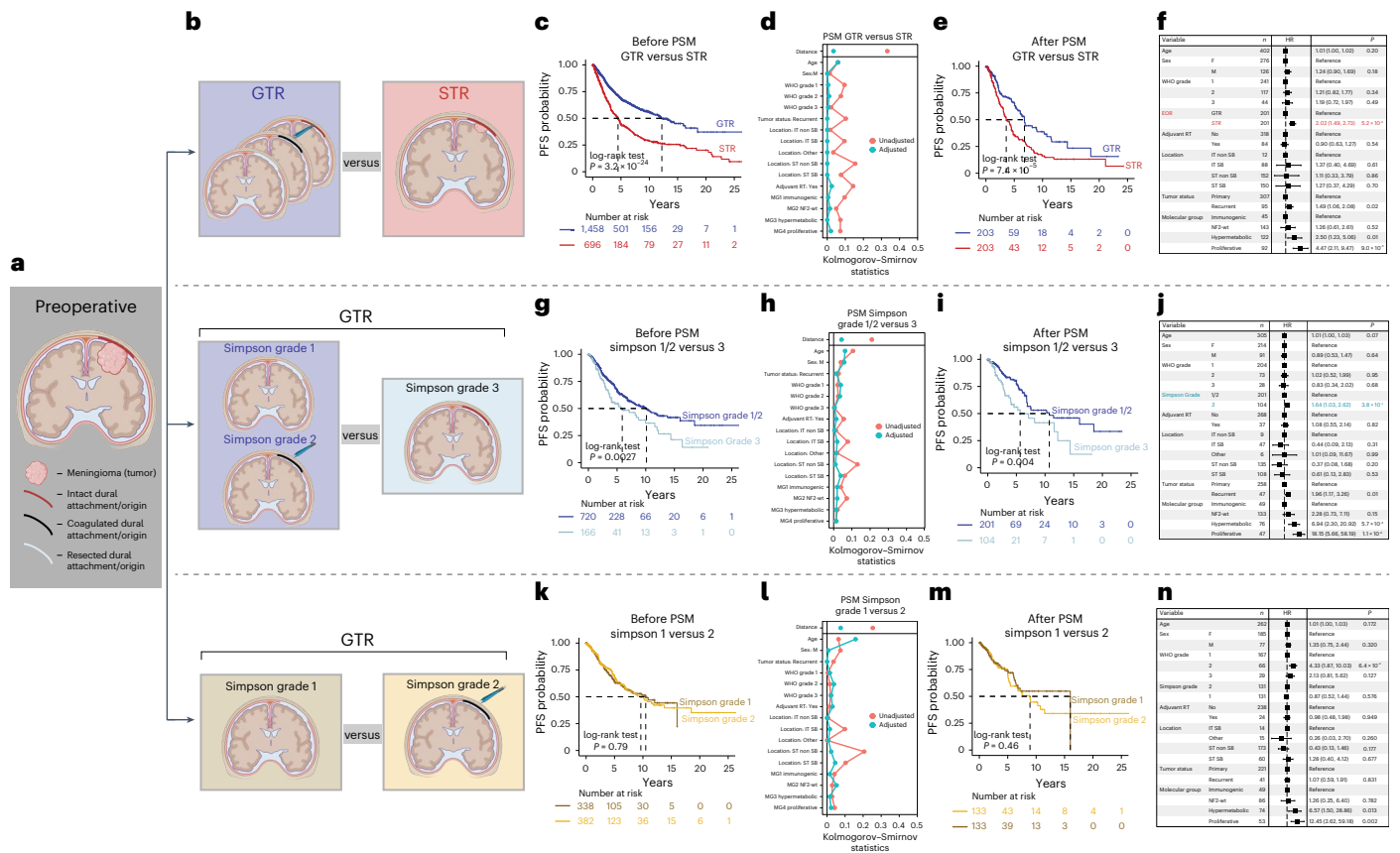


Fig. 2 | Propensity score matched analysis of degrees of surgical resection in meningioma. **a**, Schematic of a meningioma and its dural attachments/origin preoperatively, with legend indicating different methods of dural margin treatment (Simpson grades 1–3). **b**, Schematic of treatment arms being compared in PSM analyses: GTR versus STR (above), Simpson grades 1/2 versus grade 3 (middle) and Simpson grade 1 versus grade 2 (below). **c–f**, Kaplan–Meier survival plot of PFS before PSM (**c**) and covariate balance before PSM (unadjusted) and after PSM (adjusted) (**d**); Kaplan–Meier survival plot of PFS after PSM (**e**); and results of multivariable Cox regression model of PFS for GTR versus STR comparison (**f**). **g–j**, Kaplan–Meier survival plot of PFS before PSM (**g**); covariate balance before PSM (unadjusted) and after PSM (adjusted)

(**h**); Kaplan–Meier survival plot of PFS after PSM (**i**); and results of multivariable Cox regression model of PFS for Simpson grade 1/2 versus grade 3 comparison (**j**). **k–n**, Kaplan–Meier survival plot of PFS before PSM (**k**); covariate balance before PSM (unadjusted) and after PSM (adjusted) (**l**); Kaplan–Meier survival plot of PFS after PSM (**m**); and results of multivariable Cox regression model of PFS for Simpson grade 1 versus grade 2 comparison (**n**). Horizontal error bars in the forest plots of **f**, **j**, and **n** represent the 95% CI of the HRs for each of the covariates included in the multivariable Cox regressions. *P* values for each covariate in the multivariable Cox regression were derived from Wald’s test (two-tailed) without adjustments for multiple comparisons. Panels **a** and **b** were created with BioRender.

RT biomarker discovery in the RTOG-0539 meningiomas

In addition to validating RT results from the retrospective cohort above, the prospective RTOG-0539 trial cases were also utilized to discover new DNA methylation and gene expression biomarkers of RT response, given their uniform RT treatment plans and standardized outcome measures.

First, a DNA methylation-based model of RT response was trained using probes that were differentially methylated between the RTOG-0539 meningiomas that did and did not recur after RT within a 3-year window. This model was tested in two independent validation cohorts comprised of RT-treated meningiomas from the retrospective cohort (*n* = 154 and *n* = 122, respectively; Fig. 5a–e). This DNA methylation model was able to predict 3-year PFS after RT significantly more accurately than a model trained using standard-of-care WHO grade alone (*P* = 0.043, paired two-tailed DeLong’s test; Fig. 5b,d) and WHO grade combined with other clinical covariates (Extended Data Fig. 7a,e–g). Additionally, this model was able to stratify RT-treated meningiomas into an ‘RT-resistant’ and an ‘RT-responsive’ group even for tumors within each WHO grade (Fig. 5c,e and Extended Data Fig. 7c,d). Given its design, this predictive DNA methylation model is intended to be specifically utilized for RT-treated meningiomas (to predict PFS following surgery and fractionated RT) and is made publicly available for use and testing at <https://www.meningiomaconsortium.com/models/>.

Next, a gene expression-based model of RT response was trained using analogous RT-treated meningiomas from the RTOG-0539 clinical trial. First, differential RNA-seq analysis uncovered 26 differentially expressed genes among meningioma cases that progressed after RT versus those that remained stable (false discovery rate (FDR)-adjusted *P* < 0.05, log fold change (FC) > 0.57). These 26 genes were then used to build this gene expression model of RT response (Fig. 5f and Extended Data Table 3). The RT gene expression model only marginally outperformed WHO grade (*P* = 0.371, paired two-tailed DeLong’s test) and appeared less discriminative of outcome (area under the curve (AUC) = 0.725, 95% CI: 0.633–0.817; Fig. 5i) than the RT DNA methylation model (AUC = 0.777, 95% CI: 0.682–0.873; Fig. 5i) in the same retrospective validation cohort of meningiomas with matched DNA methylation and RNA-seq data (*n* = 120) on the same tumors. Gene expression patterns in these RT-resistant meningiomas showed upregulation of cell cycle and DNA repair pathways with concomitant downregulation of cell death/apoptosis pathways (Fig. 5g,h), supportive of mechanisms underlying RT resistance.

When the predictive DNA methylation and RNA-seq signatures derived from RTOG-0539 meningiomas were combined however, model performance further improved beyond that of either model alone (0.809, 95% CI: 0.722–0.897; Fig. 5j) and significantly

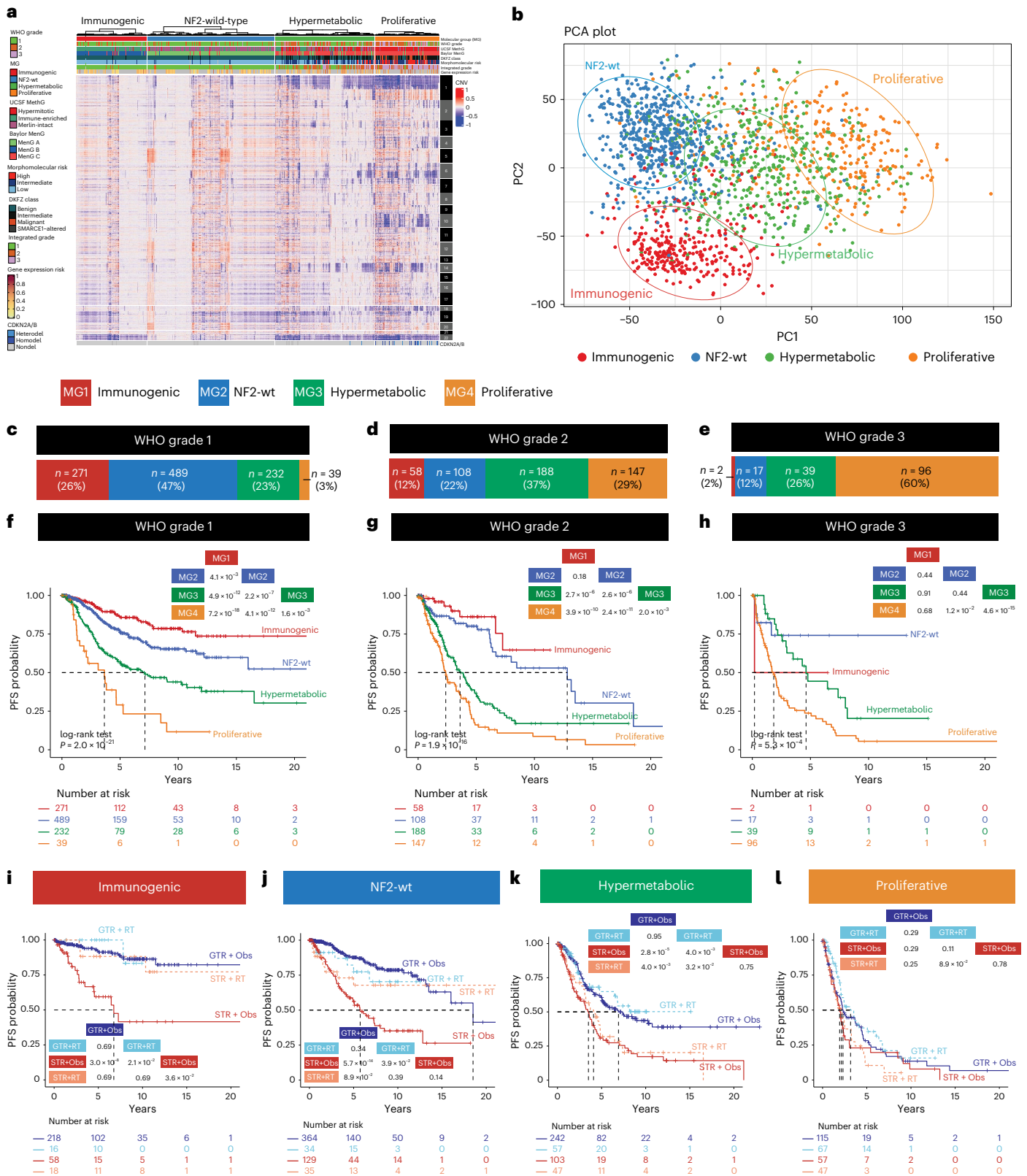


Fig. 3 | Resolution of heterogeneity in outcomes using Molecular Group classification within WHO grades. **a**, Heatmap of CNVs organized by chromosome number (vertical) and Molecular Group (MG) (horizontal) called by DNA methylation in the complete cohort of retrospective meningioma cases with available DNA methylation data. **b**, Principal component analysis (PCA) of all meningiomas based on DNA methylation, colored and circled by their respective MG. **c–e**, Molecular reclassification of meningiomas into each of the four MGs, including the proportion of cases within each respective WHO grade belonging

to each MG. **f–h**, PFS outcomes stratified by MG of meningiomas within each WHO grade: WHO grade 1 (**f**), grade 2 (**g**) and grade 3 (**h**). **i–l**, PFS outcomes stratified by EOR in molecularly defined Immunogenic (**i**), NF2-wt (**j**), Hypermetabolic (**k**) and Proliferative (**l**) meningioma cases, with PFS groups stratified based on treatment modality (EOR and receipt of adjuvant RT). Inset shows the P values from the pairwise log-rank test between groups with Benjamini-Hochberg correction for multiple comparisons. PC, principal component.

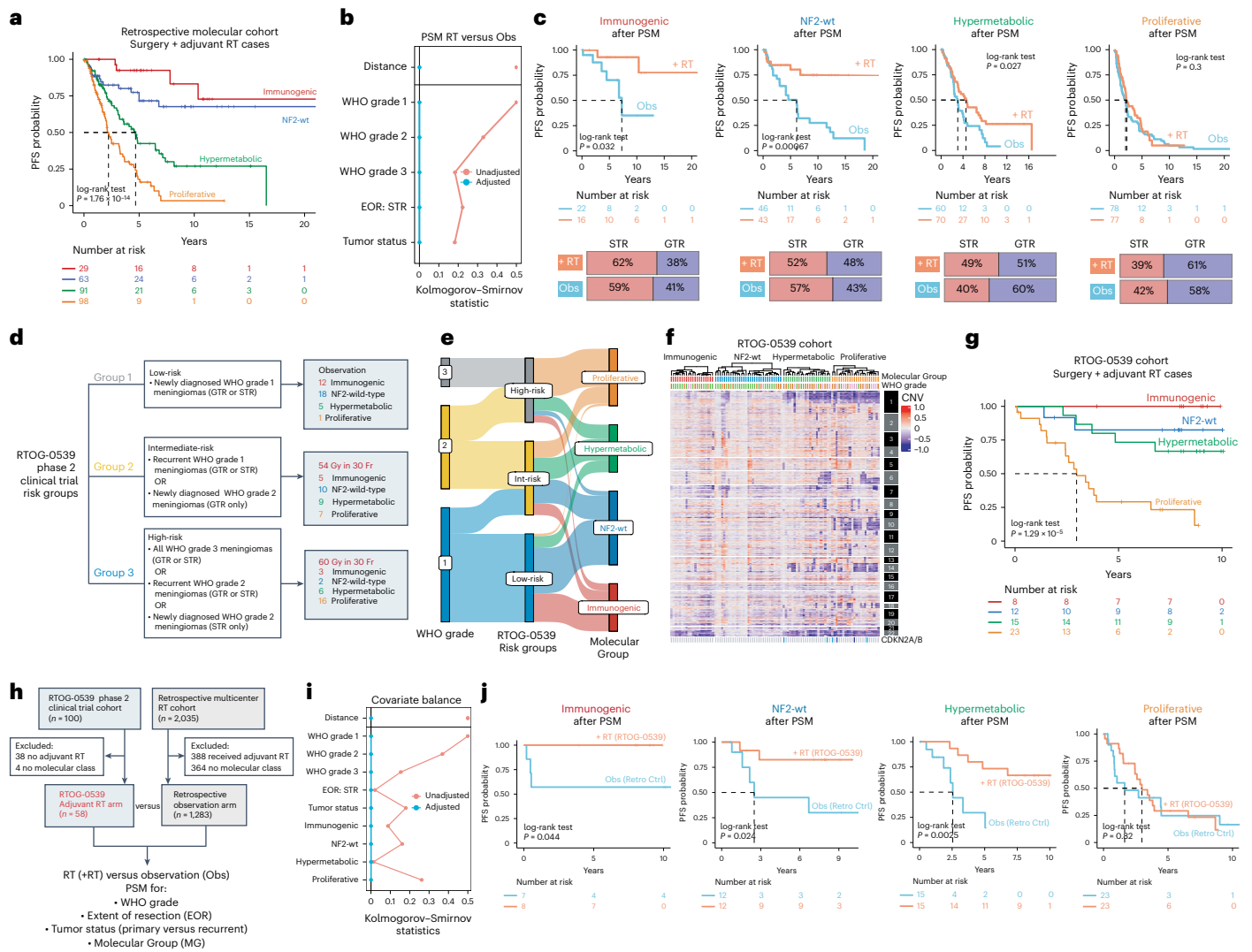


Fig. 4 | Using Molecular Group to predict response to adjuvant RT in meningiomas after surgery. **a**, PFS of cases in the retrospective molecular meningioma cohort that received adjuvant RT after surgery stratified by Molecular Group. **b**, Covariate balance before PSM (unadjusted) and after PSM (adjusted) for meningiomas treated with adjuvant RT (+RT) versus observation (Obs) after surgery. **c**, Above, PFS of the PSM retrospective cohort comparing meningiomas that received adjuvant RT (+RT) after surgery to those that were observed (Obs) in each respective Molecular Group; below, the proportion of these matched cases that received GTR and STR in each Molecular Group. **d,e**, Molecular cohort of RTOG-0539 clinical trial cases used as a validation cohort here, including their originally defined risk groups and their reclassification into Molecular Groups after molecular profiling. **f**, Genome-wide chromosomal

arm-level copy number alterations called based on DNA methylation of molecularly profiled RTOG-0539 cases organized by Molecular Group. **g**, PFS of meningiomas from the RTOG-0539 trial that received adjuvant RT after surgery (defined as the original ‘intermediate-risk’ and ‘high-risk’ treatment arms of the trial) stratified based on Molecular Group. **h**, Schematic of separate PSM analysis mimicking a randomized controlled trial with the RT arm composed entirely of RT-treated meningiomas from the prospective RTOG-0539 cohort and the control/observation arm composed of retrospective meningioma cases that did not receive adjuvant RT after surgery. **i**, Covariate balance before and after the PSM schema outlined in **k**. **j**, PFS analysis of PSM meningioma cohort stratified based on receipt of adjuvant RT (+RT; comprising only cases from the RTOG-0539 trial) versus observation (Obs; non-RTOG-0539 cases only) in each Molecular Group.

outperformed WHO grade ($P = 7.1 \times 10^{-3}$, paired two-tailed DeLong’s test). This combined molecular predictor could similarly identify RT-resistant meningiomas within each WHO grade (Fig. 5k). Median risk scores generated using this model were also significantly higher in Proliferative meningiomas than meningiomas from all other Molecular Groups, orthogonally supporting the above finding that RT-resistant meningiomas have a largely proliferative biology (Fig. 5l).

Discussion

For this study, we leveraged the largest meningioma cohort to date with multiplatform molecular, treatment and 20-year outcome data in addition to samples from a prospective phase 2 clinical trial to identify molecular predictors of treatment response in meningiomas. We used

PSM to mimic a randomized trial design to characterize the benefits of differential degrees of tumor resection and dural margin treatment across different molecular classifications, in addition to identifying a group of molecularly defined RT-resistant meningiomas. These findings have the potential to meaningfully impact clinical decision-making and treatment selection for patients in today’s molecular era of meningioma management.

Our results show that GTR imparts favorable PFS across all Molecular Groups compared to STR and although the benefits of GTR are less durable with respect to local control in more biologically aggressive meningiomas, complete resection does confer an OS benefit for these molecularly defined Proliferative meningiomas. Moreover, we show that local disease control is further improved

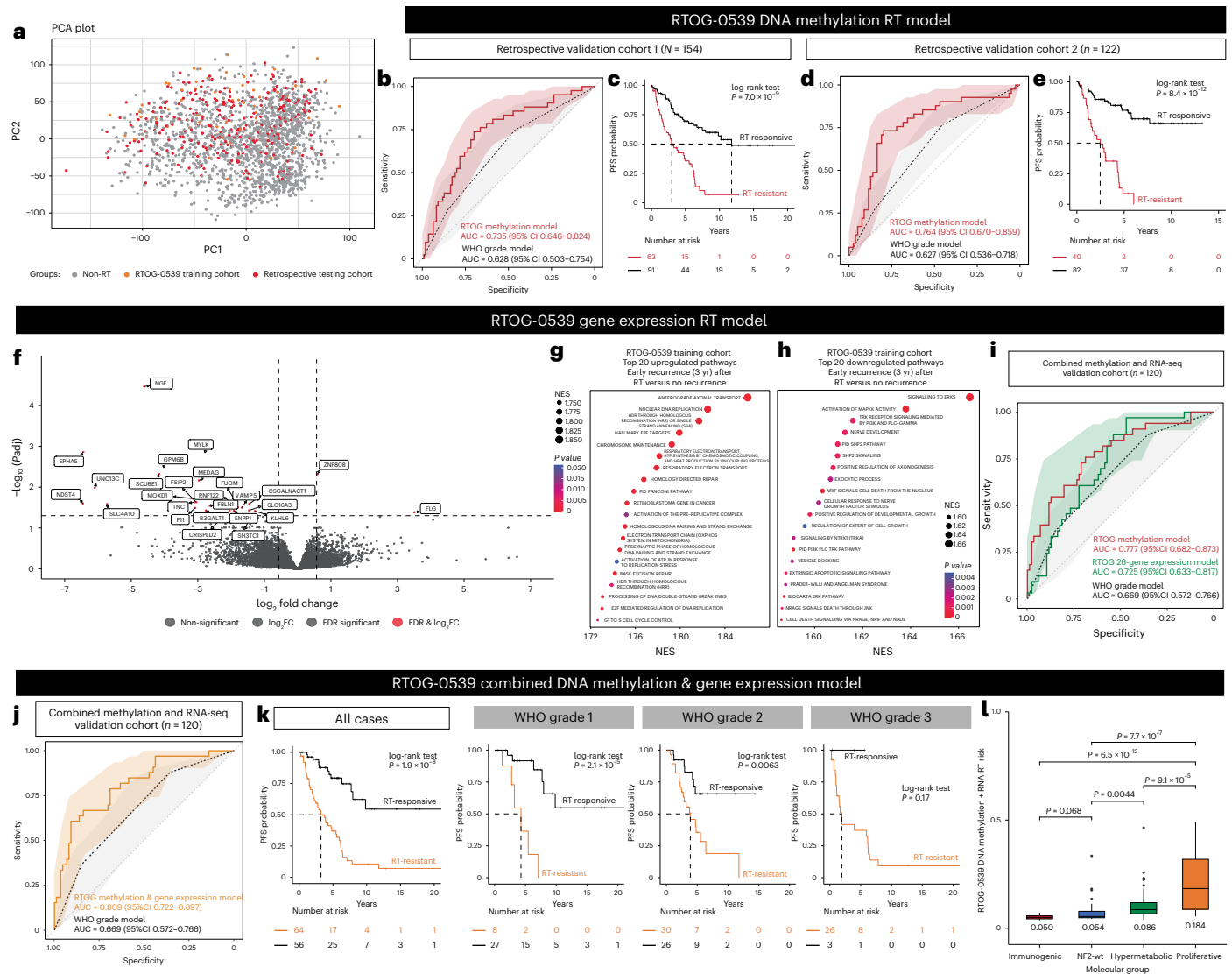


Fig. 5 | RT biomarker discovery using the RT0G-0539 clinical trial meningiomas. **a**, Principal component analysis (PCA) based on DNA methylation of meningiomas colored for model training (RT0G-0539 cohort) and model testing/validation (retrospective cohort). **b, d**, Area under the receiver operating characteristic curve (AUC ROC) and its 95% CI (shaded) for predicting 3-year PFS after RT for the RT DNA methylation model in the first (**b**) and second (**d**) retrospective validation cohorts compared to a WHO grade model. **c, e**, PFS after RT for meningiomas in the first (**c**) and second (**e**) retrospective validation cohort stratified based on RT DNA methylation risk score (high-risk and low-risk). **f**, Differential gene expression analysis on RT-treated cases in the RT0G-0539 cohort that recurred early (≤ 3 years; $n = 16$) versus cases that remained stable ($n = 46$). Labeled 26 genes met the cutoff of FDR-adjusted $P < 0.05$ (Wald’s test with Benjamini–Hochberg adjustment) and $|\log_{2}FC| > 0.57$ and were used for gene expression model building. **g, h**, The top 20 upregulated (**g**) and downregulated (**h**) gene expression pathways in the progressive RT0G-0539 meningiomas after GSEA. Unadjusted P values were obtained from permutation testing. **i**, AUC ROC and its 95% CI (shaded) for the prediction of 3-year PFS after RT for

the RT gene expression model compared to the RT DNA methylation model and a WHO grade model tested in the combined retrospective validation cohort with matched DNA methylation and RNA-seq data. **j**, AUC ROC and its 95% CI (shaded) for predicting 3-year PFS after RT for the combined RT DNA methylation and gene expression model compared to a WHO grade model tested in the same cohort. **k**, PFS of meningiomas in the combined validation cohort dichotomized into an RT-resistant and an RT-responsive group based on combined DNA methylation and gene expression risk scores and stratified across WHO grade. **l**, Distribution of predicted risk scores across Molecular Group (Immunogenic $n = 18$; NF2-wt $n = 23$; Hypermetabolic $n = 45$; Proliferative $n = 34$) generated by the combined DNA methylation and gene expression model. For all box plots, the center line shows the median risk score (annotated on the plot); the box limits are the interquartile range (IQR); and whiskers show the range of data ($Q1 - 1.5 \times IQR$, $Q3 + 1.5 \times IQR$), with additional points as outliers. P values here were obtained from two-tailed Wilcoxon rank-sum test for pairwise comparison of means between groups. NES, normalized enrichment score; PC, principal component; yr, years.

when the meningioma’s dural margin is treated either by surgical resection or thermocoagulation in addition to complete tumor resection (either Simpson grade 1 or grade 2) compared to no marginal treatment at all (Simpson grade 3), particularly for more benign Immunogenic and NF2-wt meningiomas. Notably, however, aggressive resection of dural margins (Simpson grade 1) does not appear to provide a substantial, durable benefit compared to thermocoagulation alone (Simpson grade 2). Although delineation of the ideal extent of dural resection

or coagulation to eliminate all neoplastic or pre-neoplastic disease is beyond the scope of our study, our results do suggest that the dural origin and attachments of a meningioma need to be treated in some manner to optimally delay recurrence, be it resection or cauterization. Although most treating clinicians subscribe to the maximal resection of both the meningioma and its dural attachments when possible, this had not been thoroughly investigated in a sufficiently large clinical cohort that included molecular data and the use of PSM^{8,35,36}.

The findings of our study revisit this historical dogma and provide rationale for a more nuanced consideration of addressing dural margins, particularly when it may be associated with higher surgical risk.

The effectiveness of RT for gross totally resected WHO grade 2 meningiomas is currently being investigated by the ongoing NRG-BN003 and ROAM/EORTC-1308 clinical trials. The results of these trials are expected to mature over the next several years and will be practice changing. Molecular biomarkers were not used for treatment stratification in these trials, as most relevant molecular classifications were discovered only after the inception of these studies^{37,38}. To address this gap, we leveraged the largest cohort of molecularly profiled meningiomas treated with surgery and adjuvant RT, including an invaluable cohort from the prospective RTOG-0539 phase 2 clinical trial, to show that molecular stratification of meningiomas provides predictive information beyond WHO grade when considering response to RT. Our analyses suggest that adjuvant RT provides robust PFS benefits for Immunogenic and NF2-wt meningiomas, including after incomplete resection, moderate benefit for Hypermetabolic meningiomas but little-to-no benefit for aggressive, Proliferative cases. These findings support the rationale for investigating RT results for meningiomas in the context of molecular classification and considering future molecular-pathology informed clinical trials to investigate systemic treatments for RT-resistant meningiomas.

To further define patients who might benefit from RT and to provide an individualized, probabilistic risk of tumor progression/recurrence after RT, we developed molecular models following biomarker discovery in the prospective RT-treated RTOG-0539 cases using both DNA methylation and gene expression and validated the performance of these models in independent cohorts of meningioma patients who received adjuvant RT after resection. We found that, although models using either DNA methylation or gene expression alone could outperform WHO grade in predicting response to RT, DNA methylation appeared to have better performance as a standalone platform, but a model combining both molecular modalities was optimal. These models also orthogonally supported our findings that RT-resistant meningiomas have a largely proliferative biology, enriched for cell cycle, and DNA-damage repair pathways with downregulation of apoptotic processes.

The results of this study should be considered in the context of some limitations, such as the exclusion of cases without molecular data that may be biased toward different institutions; the retrospective nature of most of the cases analyzed, including for PSM analysis, which may be ideally performed with prospective cases when available; and lack of granular data on postoperative complications, which may potentially influence outcomes and RT treatment decisions.

Online content

Any methods, additional references, Nature Portfolio reporting summaries, source data, extended data, supplementary information, acknowledgements, peer review information; details of author contributions and competing interests; and statements of data and code availability are available at <https://doi.org/10.1038/s41591-024-03167-4>.

References

- Ostrom, Q. T. et al. CBTRUS statistical report: primary brain and other central nervous system tumors diagnosed in the United States in 2015–2019. *Neuro Oncol.* **24**, v1–v95 (2022).
- Vernooij, M. W. et al. Incidental findings on brain MRI in the general population. *N. Engl. J. Med.* **357**, 1821–1828 (2007).
- Simpson, D. The recurrence of intracranial meningiomas after surgical treatment. *J. Neurol. Neurosurg. Psychiatry* **20**, 22 (1957).
- Gallagher, M. J., Jenkinson, M. D., Brodbelt, A. R., Mills, S. J. & Chavredakis, E. WHO grade 1 meningioma recurrence: are location and Simpson grade still relevant? *Clin. Neurol. Neurosurg.* **141**, 117–121 (2016).
- Gousias, K., Schramm, J. & Simon, M. The Simpson grading revisited: aggressive surgery and its place in modern meningioma management. *J. Neurosurg.* **125**, 551–560 (2016).
- Heald, J. B., Carroll, T. A. & Mair, R. J. Simpson grade: an opportunity to reassess the need for complete resection of meningiomas. *Acta Neurochir. (Wien)* **156**, 383–388 (2014).
- Nanda, A. et al. Relevance of Simpson grading system and recurrence-free survival after surgery for World Health Organization grade I meningioma. *J. Neurosurg.* **126**, 201–211 (2017).
- Sughrue, M. E. et al. The relevance of Simpson grade I and II resection in modern neurosurgical treatment of World Health Organization grade I meningiomas. *J. Neurosurg.* **113**, 1029–1035 (2010).
- Ehresman, J. S. et al. The relevance of Simpson grade resections in modern neurosurgical treatment of World Health Organization grade I, II, and III meningiomas. *World Neurosurg.* **109**, e588–e593 (2018).
- Lee, G. et al. Timing of adjuvant radiotherapy in atypical meningiomas. *Int. J. Radiat. Oncol. Biol. Phys.* **108**, S189 (2020).
- Sarhan, N. et al. Short course hypofractionated radiotherapy for frail or elderly patients with meningioma. *Cureus* **12**, e8604 (2020).
- Chen, W. C. et al. Radiotherapy for meningiomas. *J. Neurooncol.* **160**, 505–515 (2022).
- Wang, J. Z. et al. Outcomes and predictors of response to fractionated radiotherapy as primary treatment for intracranial meningiomas. *Clin. Transl. Radiat. Oncol.* **41**, 100631 (2023).
- Press, R. H. et al. Outcomes and patterns of failure for grade 2 meningioma treated with reduced-margin intensity modulated radiation therapy. *Int. J. Radiat. Oncol. Biol. Phys.* **88**, 1004–1010 (2014).
- Fleming, C. W., Parsai, S. & Suh, J. H. A management dilemma: adjuvant radiotherapy after gross total resection of atypical meningioma. *Transl. Cancer Res.* **8**, 1–3 (2019).
- Soldà, F. et al. Long-term efficacy of fractionated radiotherapy for benign meningiomas. *Radiother. Oncol.* **109**, 330–334 (2013).
- Rogers, C. L. et al. High-risk meningioma: initial outcomes from NRG Oncology/RTOG 0539. *Int. J. Radiat. Oncol. Biol. Phys.* **106**, 790–799 (2020).
- Zhu, H. et al. Efficacy of adjuvant radiotherapy for atypical and anaplastic meningioma. *Cancer Med.* **8**, 13–20 (2019).
- Maclean, J., Fersht, N. & Short, S. Controversies in radiotherapy for meningioma. *Clin. Oncol. (R. Coll. Radiol.)* **26**, 51–64 (2014).
- Lee, G. et al. Adjuvant radiation therapy versus surveillance after surgical resection of atypical meningiomas. *Int. J. Radiat. Oncol. Biol. Phys.* **109**, 252–266 (2021).
- Goldbrunner, R. et al. EANO guideline on the diagnosis and management of meningiomas. *Neuro Oncol.* **23**, 1821–1834 (2021).
- Rogers, L. et al. Intermediate-risk meningioma: initial outcomes from NRG Oncology RTOG 0539. *J. Neurosurg.* **129**, 35–47 (2018).
- Nassiri, F. et al. DNA methylation profiling to predict recurrence risk in meningioma: development and validation of a nomogram to optimize clinical management. *Neuro Oncol.* **21**, 901–910 (2019).
- Nassiri, F. et al. A clinically applicable integrative molecular classification of meningiomas. *Nature* **597**, 119–125 (2021).
- Bayley, J. C. T. et al. Multiple approaches converge on three biological subtypes of meningioma and extract new insights from published studies. *Sci. Adv.* **8**, eabm6247 (2022).
- Choudhury, A. et al. Meningioma DNA methylation groups identify biological drivers and therapeutic vulnerabilities. *Nat. Genet.* **54**, 649–659 (2022).

27. Sahm, F. et al. DNA methylation-based classification and grading system for meningioma: a multicentre, retrospective analysis. *Lancet Oncol.* **18**, 682–694 (2017).
28. Maas, S. L. N. et al. Integrated molecular-morphologic meningioma classification: a multicenter retrospective analysis, retrospectively and prospectively validated. *J. Clin. Oncol.* **39**, 3839–3852 (2021).
29. Driver, J. et al. A molecularly integrated grade for meningioma. *Neuro Oncol.* **24**, 796–808 (2021).
30. Choudhury, A. et al. Hypermitotic meningiomas harbor DNA methylation subgroups with distinct biological and clinical features. *Neuro Oncol.* **25**, 520–530 (2022).
31. Schwartz, T. H. & McDermott, M. W. The Simpson grade: abandon the scale but preserve the message. *J. Neurosurg.* **135**, 488–495 (2020).
32. Lemée, J. M. et al. Extent of resection in meningioma: predictive factors and clinical implications. *Sci. Rep.* **9**, 5944 (2019).
33. Rogers, C. L. et al. Low-risk meningioma: initial outcomes from NRG Oncology/RTOG 0539. *Neuro Oncol.* **25**, 137–145 (2023).
34. Chen, W. C. et al. Targeted gene expression profiling predicts meningioma outcomes and radiotherapy responses. *Nat. Med.* **29**, 3067–3076 (2023).
35. Ammendola, S. et al. The histopathological diagnosis of atypical meningioma: glass slide versus whole slide imaging for grading assessment. *Virchows Arch.* **478**, 747–756 (2021).
36. Nagashima, G. et al. Dural invasion of meningioma: a histological and immunohistochemical study. *Brain Tumor Pathol.* **23**, 13–17 (2006).
37. Jenkinson, M. D. et al. The ROAM/EORTC-1308 trial: radiation versus observation following surgical resection of atypical meningioma: study protocol for a randomised controlled trial. *Trials* **16**, 519 (2015).
38. Jenkinson, M. D. et al. Radiotherapy versus observation following surgical resection of atypical meningioma (the ROAM trial). *Neuro Oncol.* **16**, 1560–1561 (2014).

Publisher's note Springer Nature remains neutral with regard to jurisdictional claims in published maps and institutional affiliations.

Open Access This article is licensed under a Creative Commons Attribution-NonCommercial-NoDerivatives 4.0 International License, which permits any non-commercial use, sharing, distribution and reproduction in any medium or format, as long as you give appropriate credit to the original author(s) and the source, provide a link to the Creative Commons licence, and indicate if you modified the licensed material. You do not have permission under this licence to share adapted material derived from this article or parts of it. The images or other third party material in this article are included in the article's Creative Commons licence, unless indicated otherwise in a credit line to the material. If material is not included in the article's Creative Commons licence and your intended use is not permitted by statutory regulation or exceeds the permitted use, you will need to obtain permission directly from the copyright holder. To view a copy of this licence, visit <http://creativecommons.org/licenses/by-nc-nd/4.0/>.

© The Author(s) 2024

Justin Z. Wang^{1,2,3}, **Vikas Patil**^{1,3}, **Alexander P. Landry**^{1,2,3,95}, **Chloe Gui**^{1,2,3,95}, **Andrew Ajisebutu**^{1,3,95}, **Jeff Liu**^{1,3}, **Olli Saarela**⁴, **Stephanie L. Pugh**⁵, **Minhee Won**⁵, **Zeel Patel**⁶, **Rebeca Yakubov**^{1,3}, **Ramneet Kaloti**^{1,3}, **Christopher Wilson**⁷, **Aaron Cohen-Gadol**⁸, **Mohamed A. Zaazoue**^{9,10}, **Ghazaleh Tabatabai**^{11,12,13}, **Marcos Tatagiba**¹⁴, **Felix Behling**¹⁴, **Damian A. Almiron Bonnin**¹⁵, **Eric C. Holland**¹⁶, **Tim J. Kruser**¹⁷, **Jill S. Barnholtz-Sloan**^{18,19,20}, **Andrew E. Sloan**²¹, **Craig Horbinski**^{22,23}, **Silky Chotai**²⁴, **Lola B. Chambless**²⁴, **Andrew Gao**²⁵, **Alexander D. Rebchuk**²⁶, **Serge Makarenko**²⁶, **Stephen Yip**²⁷, **Felix Sahm**^{28,29}, **Sybren L. N. Maas**^{30,31}, **Derek S. Tsang**³², **The International Consortium on Meningiomas (ICOM)***, **C. Leland Rogers**³³, **Kenneth Aldape**³⁴, **Farshad Nassiri**^{1,2,3,96} ✉ & **Gelareh Zadeh**^{1,2,3,94,96} ✉

¹MacFeeters Hamilton Neuro-Oncology Program, Princess Margaret Cancer Centre, University Health Network and University of Toronto, Toronto, Ontario, Canada. ²Division of Neurosurgery, Department of Surgery, University of Toronto, Toronto, Ontario, Canada. ³Princess Margaret Cancer Centre, University Health Network, Toronto, Ontario, Canada. ⁴Dalla Lana School of Public Health, University of Toronto, Toronto, Ontario, Canada. ⁵NRG Oncology Statistics and Data Management Center, Philadelphia, PA, USA. ⁶Temerty School of Medicine, University of Toronto, Toronto, Ontario, Canada. ⁷Neurosurgery Specialists of Tulsa, Tulsa, OK, USA. ⁸Department of Neurological Surgery, Keck School of Medicine of the University of Southern California, Los Angeles, CA, USA. ⁹Department of Neurological Surgery, Indiana University School of Medicine, Indianapolis, IN, USA. ¹⁰Department of Orthopedic Surgery, Washington University School of Medicine in St. Louis, St. Louis, MO, USA. ¹¹German Cancer Consortium (DKTK), DKFZ Partner Site Tübingen, Tübingen, Germany. ¹²Cluster of Excellence (EXC 2180) 'Image Guided and Functionally Instructed Tumor Therapies', Eberhard Karls University Tübingen, Tübingen, Germany. ¹³Department of Neurology and Interdisciplinary Neuro-Oncology, Center for Neuro-Oncology, Comprehensive Cancer Center, Hertie Institute for Clinical Brain Research, Eberhard Karls University Tübingen, Tübingen, Germany. ¹⁴Department of Neurosurgery, Center for Neuro-Oncology, Comprehensive Cancer Center, Eberhard Karls University Tübingen, Tübingen, Germany. ¹⁵Department of Pathology, University of San Francisco, San Francisco, CA, USA. ¹⁶Human Biology Division, Fred Hutchinson Cancer Center, Seattle, WA, USA. ¹⁷Department of Human Oncology, University of Wisconsin Hospitals and Clinics, Madison, WI, USA. ¹⁸Central Brain Tumor Registry of the United States, Hinsdale, IL, USA. ¹⁹Trans Divisional Research Program (TDRP), Division of Cancer Epidemiology and Genetics (DCEG), National Cancer Institute, Bethesda, MD, USA. ²⁰Center for Biomedical Informatics & Information Technology (CBIIIT), National Cancer Institute, Bethesda, MD, USA. ²¹Piedmont Brain Tumor Center, Piedmonth Healthcare System, Atlanta, GA, USA. ²²Department of Pathology, Northwestern University, Evanston, IL, USA. ²³Lou & Jean Malnati Brain Tumor Institute at the Lurie Comprehensive Cancer Center, Northwestern University, Evanston, IL, USA. ²⁴Department of Neurosurgery, Vanderbilt University Medical Center, Nashville, TN, USA. ²⁵Department of Laboratory Medicine and Pathobiology, University of Toronto, Toronto, Ontario, Canada. ²⁶Division of Neurosurgery, University of British Columbia, Vancouver, British Columbia, Canada. ²⁷Department of Pathology & Laboratory Medicine, Faculty of Medicine, University of British Columbia, Vancouver, British Columbia, Canada. ²⁸Department of Neuropathology, Institute of Pathology, Ruprecht-Karls-University Heidelberg, Heidelberg, Germany. ²⁹Clinical Cooperation Unit Neuropathology, German Cancer Research Center (DKFZ), Heidelberg, Germany. ³⁰Department of Pathology, Leiden University Medical Center, Leiden, The Netherlands. ³¹Department of Pathology, Erasmus MC Cancer Institute, University Medical Center Rotterdam, Rotterdam, The Netherlands. ³²Radiation Medicine Program, Princess Margaret Cancer Centre, Toronto, Ontario, Canada. ³³Radiation Oncology, Utah Cancer Specialists, Salt Lake City, UT, USA. ³⁴Center for Cancer Research, National Cancer Institute, Bethesda, MD, USA.

⁹⁴Arthur and Sonia Labatt Brain Tumour Research Centre, The Hospital for Sick Children, Toronto, Ontario, Canada. ⁹⁵These authors contributed equally: Alexander P. Landry, Chloe Gui, Andrew Ajisebutu. ⁹⁶These authors jointly supervised this work: Farshad Nassiri, Gelareh Zadeh. *A list of authors and their affiliations appears at the end of the paper. ✉e-mail: farshad.nassiri@uhn.ca; gelareh.zadeh@uhn.ca

The International Consortium on Meningiomas (ICOM)

Farshad Nassiri^{1,2,3,96}, Justin Z. Wang^{1,2,3}, Alexander P. Landry^{1,2,3,95}, Gelareh Zadeh^{1,2,3,94,96}, Michael W. McDermott³⁵, Thomas Santarius³⁶, Warren Selman³⁷, Marta Couce³⁸, Andrew E. Sloan²¹, Bruno Carvalho³⁹, Patrick Y. Wen⁴⁰, Kyle M. Walsh⁴¹, Sybren L. N. Maas^{30,31}, Eelke M. Bos⁴², Wenya Linda Bi⁴³, Raymond Y. Huang⁴⁴, Priscilla K. Brastianos⁴⁵, Helen A. Shih⁴⁶, Tobias Walbert⁴⁷, Ian Lee⁴⁸, Michelle M. Felicella⁴⁹, Ana Valeria Castro⁴⁸, Houtan Noushmehr⁴⁸, James M. Snyder⁴⁸, Aaron Cohen-Gadol⁸, Francesco Dimeco⁵⁰, Andrea Saladino⁵⁰, Bianca Pollo⁵¹, Christian Schichor⁵², Jörg-Christian Tonn⁵², Felix Ehret⁵³, Timothy J. Kaufmann⁵⁴, Daniel H. Lachance⁵⁵, Caterina Giannini⁵⁵, Evanthia Galanis⁵⁶, Aditya Raghunathan⁵⁵, Michael A. Vogelbaum⁵⁷, Kenneth Aldape³⁴, Jill Barnholtz-Sloan^{18,19,20}, Patrick J. Cimino⁵⁸, Craig M. Horbinski^{22,23}, Mark Youngblood⁵⁹, Matija Snuderl⁶⁰, Sylvia C. Kurz¹³, Erik P. Sulman⁶¹, Ian F. Dunn⁶², C. Oliver Hanemann⁶³, Mohsen Javadpour⁶⁴, Ho-Keung Ng⁶⁵, Paul C. Boutros⁶⁶, Richard G. Everson⁶⁷, Alkiviadis Tzannis⁶⁸, Konstantinos N. Fountas⁶⁸, Nils Ole Schmidt⁶⁹, Karolyn Au⁷⁰, Roland Goldbrunner⁷¹, Norbert Galldiks⁷², Marco Timmer⁷³, Tiit Illimar Mathiesen⁷⁴, Manfred Westphal⁷⁵, Katrin Lamszus⁷⁵, Franz L. Rieckels⁷⁵, Christel Herold-Mende⁷⁶, Felix Sahm²⁸, Christine Jungk⁷⁶, Gerhard Jungwirth⁷⁶, Andreas von Deimling²⁸, Maximilian Deng⁷⁷, Susan C. Short⁷⁸, Michael D. Jenkinson⁷⁹, Christian Mawrin⁸⁰, Abdurrahman I. Islam⁸¹, Daniel M. Fountain³⁶, Omar N. Pathmanaban⁸¹, Katharine J. Drummond⁸², Andrew Morokoff⁸², David R. Raleigh^{83,84,85}, Arie Perry⁸⁵, Nicholas A. Butowski⁸⁴, Tathiane M. Malta⁸⁶, Viktor Zherebitskiy⁸⁷, Luke Hnenny⁸⁸, Gabriel Zada⁸⁹, Ghazaleh Tabatabai^{11,12,13}, Felix Behling¹⁴, Mirjam Renovanz¹⁴, Marcos Tatagiba¹⁴, Antonio Santacrose⁹⁰, Christian la Fougère⁹¹, Jens Schittenhelm¹⁴, Paul Passlack^{13,14}, Stephen Yip²⁷, Serge Makarenko²⁶, Jennifer Moliterno⁹² & Alper Dincer⁹³

³⁵Miami Neuroscience Institute, Baptist Health, Miami, FL, USA. ³⁶Department of Neurosurgery, Addenbrooke's Hospital, Cambridge, UK. ³⁷Department of Neurosurgery, University Hospitals Cleveland and Case Western Reserve University, Cleveland, OH, USA. ³⁸Department of Pathology, University Hospitals Case Medical Center, Cleveland, OH, USA. ³⁹Department of Neurosurgery, Centro Hospitalar Universitário S. João, Porto, Portugal. ⁴⁰Center for Neuro-Oncology, Dana-Farber/Brigham and Women's Cancer Center, Boston, MA, USA. ⁴¹Department of Neurosurgery, Duke University, Durham, NC, USA. ⁴²Department of Neurosurgery, Erasmus MC Cancer Institute, Erasmus University Medical Center, Rotterdam, The Netherlands. ⁴³Department of Neurosurgery, Brigham and Women's Hospital, Harvard Medical School, Boston, MA, USA. ⁴⁴Department of Radiology, Brigham and Women's Hospital, Dana-Farber Cancer Institute, Harvard Medical School, Boston, MA, USA. ⁴⁵Department of Neurology, Division of Neuro-Oncology, Massachusetts General Hospital, Harvard Medical School, Boston, MA, USA. ⁴⁶Department of Radiation Oncology, Massachusetts General Hospital, Boston, MA, USA. ⁴⁷Department of Neurology, Hermelin Brain Tumor Center, Henry Ford Health, Detroit, MI, USA. ⁴⁸Department of Neurosurger, Hermelin Brain Tumor Center, Henry Ford Health, Detroit, MI, USA. ⁴⁹Department of Pathology, University of Texas Medical Branch, Galveston, TX, USA. ⁵⁰Department of Neurosurgery, Fondazione IRCCS Istituto Neurologico Carlo Besta, Milan, Italy. ⁵¹Neuropathology Unit, Fondazione IRCCS Istituto Neurologico Carlo Besta, Milan, Italy. ⁵²Department of Neurosurgery, LMU University Hospital, LMU Munich, Munich, Germany. ⁵³Department of Radiation Oncology, Charité – Universitätsmedizin Berlin, Corporate Member of Freie Universität Berlin and Humboldt-Universität zu Berlin, Berlin, Germany. ⁵⁴Department of Radiology, Mayo Clinic, Rochester, MN, USA. ⁵⁵Department of Laboratory Medicine and Pathology, Mayo Clinic, Rochester, MN, USA. ⁵⁶Department of Oncology, Division of Medical Oncology, Mayo Clinic, Rochester, MN, USA. ⁵⁷Departments of Neuro-Oncology and Neurosurgery, Moffitt Cancer Center, Tampa, FL, USA. ⁵⁸Neuropathology Unit, Surgical Neurology Branch, National Institute of Neurological Disorders and Stroke, National Institutes of Health, Bethesda, MD, USA. ⁵⁹Department of Neurological Surgery, Northwestern University, Northwestern Medicine, Chicago, IL, USA. ⁶⁰Department of Pathology, NYU Langone Medical Center, New York, NY, USA. ⁶¹Department of Radiation Oncology, NYU Langone Health, New York University, New York, NY, USA. ⁶²Department of Neurosurgery, University of Oklahoma Health Sciences Center, Oklahoma City, OK, USA. ⁶³Peninsula Schools of Medicine and Dentistry, Plymouth University, Plymouth, UK. ⁶⁴Department of Neurosurgery, Royal College of Surgeons in Ireland, Dublin, Ireland. ⁶⁵Department of Anatomical and Cellular Pathology, Chinese University of Hong Kong, Shatin, Hong Kong. ⁶⁶Department of Human Genetics, University of California, Los Angeles, Los Angeles, CA, USA. ⁶⁷Department of Neurosurgery, University of California, Los Angeles, Los Angeles, USA. ⁶⁸Department of Neurosurgery, University Hospital of Larissa, School of Medicine, University of Thessaly, Larissa, Greece. ⁶⁹Department of Neurosurgery, University Medical Center Regensburg, Regensburg, Germany. ⁷⁰Department of Surgery, Division of Neurosurgery, University of Alberta, Edmonton, Alberta, Canada. ⁷¹Center of Neurosurgery, Department of General Neurosurgery, University of Cologne, Cologne, Germany. ⁷²Department of Neurology, Faculty of Medicine, University Hospital Cologne, University of Cologne, Cologne, Germany. ⁷³Laboratory for Neurooncology and Experimental Neurosurgery, Department of General Neurosurgery, Center for Neurosurgery, Cologne, Germany. ⁷⁴Department of Neurosurgery, University Hospital of Copenhagen-Rigshospitalet, Copenhagen, Denmark. ⁷⁵Department of Neurosurgery, University Medical Center Hamburg-Eppendorf, Hamburg, Germany. ⁷⁶Department of Neurosurgery, University Hospital Heidelberg, Heidelberg, Germany. ⁷⁷Department of Radiation Oncology, Heidelberg University Hospital, Heidelberg, Germany. ⁷⁸Leeds Institute of Medical Research at St. James's, University of Leeds, Leeds, UK. ⁷⁹Department of Neurosurgery, The Walton Centre NHS Foundation Trust, Liverpool, UK. ⁸⁰Institute of Neuropathology, Otto-Von-Guericke-University, Magdeburg, Germany. ⁸¹Department of Neurosurgery, Manchester Centre for Clinical Neurosciences, Salford Royal Hospital NHS Foundation Trust, Salford, UK. ⁸²Department of Neurosurgery, Royal Melbourne Hospital, Melbourne, VIC, Australia. ⁸³Department of Radiation Oncology, University of California, San Francisco, San Francisco, CA, USA. ⁸⁴Department of Neurosurgery, University of California, San Francisco, San Francisco, CA, USA. ⁸⁵Department of Pathology, University of California, San Francisco, San Francisco, CA, USA. ⁸⁶School of Pharmaceutical Sciences of Ribeirão, Preto University of São Paulo, São Paulo, Brazil. ⁸⁷Department of Pathology and Laboratory Medicine, University of Saskatchewan College of Medicine, Saskatoon, Saskatchewan, Canada. ⁸⁸Division of Neurosurgery, Royal University Hospital, University of Saskatchewan, Saskatoon, Saskatchewan, Canada. ⁸⁹USC Pituitary Center, USC Radiosurgery Center, Keck School of Medicine of USC, Los Angeles, CA, USA. ⁹⁰Department of Neurosurgery, St. Barbara-Klinik Hamm-Heessen, Hamm, Germany. ⁹¹Nuclear Medicine and Clinical Molecular Imaging, Department of Radiology, Eberhard Karls University of Tübingen, Tübingen, Germany. ⁹²Department of Neurosurgery, Yale School of Medicine, New Haven, CT, USA. ⁹³Department of Neurosurgery, Tufts Medical Center, Boston, MA, USA.

Methods

Clinical cohort

Clinical data were collected for patients with meningiomas from 10 different participating institutions of the International Consortium on Meningiomas (ICOM) by expert clinicians, including neurosurgeons, neurooncologists and radiation oncologists, specializing in the treatment of meningiomas at their respective institution. Meningiomas were operated on between 2000 and 2020 and enriched for clinical aggressiveness or higher WHO grade tumors. Specific data elements collected were in accordance with pre-established common data elements designed for studies on meningiomas and included age, sex, tumor status (recurrent or primary at the time of surgery), WHO grade, Simpson grade, receipt of adjuvant RT, histological subtype and location³⁹. Meningiomas were graded by experienced neuropathologists from each institution in accordance with either the 2016 or the 2021 WHO classification, and central pathological review was performed at the University Health Network in Toronto, Canada, when slides or tissue were available. Data from additional publicly available repositories were also collected. All meningiomas with molecular data were centrally re-graded in accordance with 2021 WHO classification based on the presence of *CDKN2A/B* homozygous deletion or *TERT* p mutation (Supplementary Table 27)⁴⁰. Our primary outcome was PFS, defined as the time from the index surgery to the time that progression or recurrence was seen on imaging noted by either the reporting neuro-radiologist at each respective institution or another treating clinician, death from any cause if the patient died without documentation of progression or the last date of neurosurgical or radiographic follow-up if the patient was subsequently lost to follow-up. Secondary outcome was OS, defined as the date from the index surgery to either the date of confirmed death or date of last follow-up, at which point the patient was censored if death was not confirmed. Meningiomas without data on WHO grade, clinical follow-up to determine PFS or OS or documented EOR were excluded (Fig. 1a). The NRG Oncology RTOG-0539 (NCT00895622) is a prospective, phase 2, non-randomized clinical trial with fully mature clinical follow-up data that stratified patients with meningiomas to adjuvant RT or observation treatment arms. In this trial, patients were divided into low-risk, intermediate-risk and high-risk groups based on WHO grade, primary/recurrent tumor status and EOR. Patients in the low-risk group were managed with observation, whereas those in the intermediate-risk and high-risk groups were treated with uniform RT protocols after surgery^{17,22,33}. Tissue for molecular profiling and clinical data from the RTOG-0539 trial were obtained through the Molecular Profiling to Predict Response to Treatment (MP2PRT) program as part of the National Cancer Institute's Cancer Moonshot Initiative. Ethics approval for this study was provided by the Research Ethics Board via the Coordinated Approval Process for Clinical Research at the University Health Network (Toronto, Canada) locally under CAPCR18-5820 and by relevant institutional review boards (IRBs) at all included institutions (Indiana University, Case Western Reserve University, University of Tübingen, Vanderbilt University, Vancouver General Hospital, Fred Hutchinson Cancer Center and Northwestern University). As part of institutional policy and routine surgical consent, patients whose meningiomas were included in this study provided consent for their tumor sample, tumor data and de-identified clinical data to be used for clinical or translational research projects.

EOR

EOR was reported by the treating, experienced neurosurgeon at each respective institution as either GTR, indicating complete macroscopic removal of the tumor with or without dural coagulation or excision, or STR, indicating residual macroscopic tumor postoperatively. Post-operative magnetic resonance imaging (MRI) scans were reviewed centrally by experienced neuroradiologists for all Toronto cases with EOR data ($n = 358$). When available, postoperative radiographic imaging was reviewed within each institution to verify EOR ($n = 680$).

In the remainder of cases with documented EOR, including for publicly available datasets ($n = 769$), it was indeterminate whether post-operative MRI was reviewed to confirm the surgeons' impression. More granular reporting of Simpson grade was also performed based on the reporting surgeon on whether the overlying dura was excised completely (Simpson grade 1), thermocoagulated (Simpson grade 2) or left in situ without either of these measures performed (Simpson grade 3). For equivocal cases, the Simpson grade was omitted and these cases were not included in Simpson grade analyses. All meningiomas that underwent STR were designated as Simpson grade 4, and all tumors where only a biopsy was performed for tissue diagnosis (Simpson grade 5) were excluded.

DNA and RNA extraction

DNA and RNA were extracted from a combination of fresh-frozen and paraffin-embedded tissue for meningiomas using a DNeasy Blood and Tissue kit (QIAGEN, 69506), a QIAamp DNA FFPE Tissue kit (QIAGEN, 56404), a RNeasy Mini kit (QIAGEN, 74104) and an AllPrep DNA/RNA FFPE kit (QIAGEN, 80234) and quantified using a NanoDrop 1000 instrument (Thermo Fisher Scientific) and an Agilent Bioanalyzer (Agilent Technologies).

DNA methylation

The Illumina Infinium MethylationEPIC BeadChip array (Illumina) was used to obtain genome-wide DNA methylation profiles on 250–500 ng of DNA after bisulfite conversion with an EZ DNA Methylation kit (Zymo Research, D5002). General quality control (QC) measures were performed as previously described and in accordance with the manufacturer's instructions. Processing of methylation files (IDAT) was performed as previously described using the University of California Santa Cruz Genome Browser (GRCh38/hg38 assembly) and the minfi package (Bioconductor v.1.46.0). Differentially methylated probes/CpGs were identified using the limma package in Bioconductor⁴¹.

RNA-seq

cDNA libraries were generated as previously described on RNA samples that passed standard QC measures on the Agilent Bioanalyzer and sequenced on an Illumina NovaSeq 6000 S4 flow cell (paired end 2×150 base pairs (bp)) to obtain 70 million reads per sample. The quality of raw reads was initially assessed using FastQC (v.0.11.5)^{42,43}. After this, adaptors were trimmed using Trim Galore (v.0.5.0)⁴⁴. Next, STAR aligner (v.2.4.2a) was used to align reads to the human reference genome (hg38), and, subsequently, HtSeq (v.0.11.0) was employed to count reads over gene exons^{45,46}. Gene annotation was then carried out using GENCODE (v.33)⁴⁷.

Copy number alterations

Copy number alterations for each tumor were inferred from their DNA methylation data using the conumee package in Bioconductor, as previously described^{48,49}. Chromosomal arm-level CNVs were called based on the average \log_2 ratio of methylated and unmethylated probe intensities across the entire arm with < -0.2 as a 'loss', > 0.2 as a 'gain' and otherwise as 'neutral'. All losses and gains were manually confirmed by independent visual inspection of the genome-wide CNV plot. Homozygous loss of *CDKN2A/B* was determined by manual inspection of the genome-wide CNV plots for each sample as previously described, and cases were upgraded to 'WHO grade 3' where homozygous loss was present in accordance with the 2021 WHO classification criteria for meningiomas^{40,50,51}.

TERTp sequencing

Amplification of the *TERT* promoter region containing the hotspots C228T and C250T was performed on 973 meningioma tumor samples. *TERT* p mutation status was available for an additional 109 cases from

the previously published study by Bayley et al.²⁵. Platinum SuperFi II PCR Master Mix (Thermo Fisher Scientific, 12368010) with primers 5'-AGTGGATTCGCGGGCACAGA-3' and 5'-CAGCGCTGCCTGAACTC-3' was used to produce a 235-bp amplicon⁵². Polymerase chain reaction (PCR) products were separated by gel electrophoresis to verify a product at the correct size. After purification with a ZR-96 DNA Clean-Up kit (Zymo Research, D4018), PCR products were sent for Sanger sequencing at the Centre for Applied Genomics (Toronto, Canada). Chromatograms were analyzed in Geneious Prime, and all C228T and C250T mutations were confirmed by sequencing of a second PCR reaction⁵³.

Molecular Group stratification

The DKFZ methylation class (benign, intermediate and malignant) and subclasses (benign-1, benign-2, benign-3, intermediate-A, intermediate-B, malignant and SMARCE1-altered) were determined for each tumor through manually inputting IDAT files generated through DNA methylation into the publicly accessible brain tumor classifier v.12.5 (<https://www.molecularneuropathology.org/mnp/>)²⁷. For cases that had a classification calibrated score below 0.80, a *t*-distributed stochastic neighbor embedding (*t*-SNE; Rtsne R package (v.0.16)) and a uniform manifold approximation and projection (UMAP) were plotted using reference cases from the brain tumor classifier v11.4 and institutional meningioma samples to confirm sample clustering with other known meningioma reference cases. Cases that did not classify or cluster with meningiomas in this manner or that classified or clustered with other pathologies (for example, solitary fibrous tumor/hemangiopericytoma and inflammatory cortex) were excluded from downstream molecular classification. For primary analysis, meningiomas were assigned to the four Molecular Groups originally published by Nassiri et al.²⁴—Immunogenic (MG1), NF2-wt (MG2), Hypermetabolic (MG3) and Proliferative (MG4)—using a combination of DNA methylation, CNV and gene expression data (where available)²⁴. The former two groups consist of predominantly benign meningiomas, whereas the latter two groups are enriched for clinically aggressive meningiomas. For sensitivity analyses, meningiomas were also assigned to other methylation/molecular classifications previously published by Sahm et al., Choudhury et al. and Bayley et al. based on the original methodologies described in each respective publication and confirmed using multiple, independent orthogonal approaches (Extended Data Figs. 1 and 2)^{24–26,28,29,34,54}. In brief, DNA methylation was used to derive the UCSF MethG and Baylor MenG. Additional confirmation of the fidelity of each tumor's molecular classification was performed using three additional, common methods. First, a multinomial elastic net (GLMnet) classifier was trained on the cohort from which the original molecular classification was derived from using DNA methylation and RNA-seq data where available and then applied to all other datasets from the other cohorts to predict the probability of each sample belonging to a specific molecular class or group⁵⁵. Next, non-negative matrix factorization (NMF R package (v.0.27)) was used to extract metagenes from the DNA methylation and RNA-seq data of each of the original molecular classification's training cohort and applied these metagene signatures to cluster all other samples into molecular/methylation groups^{56,57}. In rare instances where there were discrepancies between the predicted molecular/methylation groups across any of these methodologies, two independent blinded reviewers (V.P. and A.P.L.) manually examined the CNV plots and determined a consensus classification based on the degree of changes pathognomic to each molecular/methylation group (for example, chr 1p loss, 14 loss, 10 loss, 5 gain, 12 gain, 22q loss and *CDKN2A/B* deletion). Meningiomas were also stratified to the following three integrated molecular prognostic systems—Integrated Grade, Morphomolecular Risk Group and Gene Expression Risk—based on the methodologies described in each group's original publication^{28,29,34}. For the former two prognostic systems that integrate chromosomal arm-level CNVs into classification, losses and gains of respective chromosomal arms were defined

based on the cutoffs specified above (see 'Copy number alterations' subsection) and confirmed by manual inspection of the genome-wide CNV plots. Chromosomal arm-level changes were defined as 'gain', 'loss' or 'neutral', and points were allocated for specific losses in keeping with what was previously published for Integrated Grade and Morphomolecular Risk Group. Even partial chromosomal arm losses or gains were considered, in keeping with previous reports⁵⁴. For Gene Expression Risk, only cases with available RNA-seq (including all cases with matched DNA methylation) were able to be used. The Gene Expression model was trained in the publicly available UCSF cohort ($n = 185$), using their methodologies as originally published, by computing the product of the LASSO regularized Cox regression coefficient (from the *glmnet* and *cv.glmnet* functions of the *glmnet* package (v.4.1-8) in R) of the predefined 34-gene signature and the normalized counts of the 34 prognostic genes⁵⁵. This value was then rescaled from 0 to 1 to define a probabilistic risk metric. Bootstrap aggregation was used to train 500 ridge-regression submodels to determine a bootstrap aggregated risk score for each training sample, and these risk scores were then applied to the validation cohorts with available RNA-seq data³⁴.

PSM

PSM was performed using a 1:1 or 2:1 (when Simpson grades 1 and 2 were grouped together to compare to Simpson grade 3) nearest neighbor matching algorithm without replacement with a predefined caliper width ranging from 0.10 to 0.20. PSM was performed based on the same following variables unless otherwise defined in the text: age, sex, WHO grade, primary/recurrent tumor status, receipt of adjuvant RT, tumor location and one of each of the respective molecular classification schemes (Molecular Group, UCSF MethG and Baylor MenG) and integrated molecular prognostic systems (Integrated Grade, Morphomolecular Risk and Gene Expression Risk)^{24–26,28,29,34}. Covariate balance was assessed by computing the standardized mean difference after PSM. To address missing clinical data (non-outcome and non-molecular data), multiple imputation was performed using the 'mice' package in R to impute five separate complete datasets; PSM was performed within each imputed dataset followed by averaging the treatment effects of a multivariable Cox regression within each dataset; and then the Rubin formula was used to combine estimates from these multiply imputed full datasets into a single set of results (results of the pooled Cox multivariable model) using the MatchThem package in R^{58,59}.

RT DNA methylation model building

Meningiomas from the intermediate-risk and high-risk groups of the prospective RTOG-0539 trial were used to develop molecular models capable of accurately predicting response to RT on an individual patient level^{17,22}. These tumors received consistent and uniform adjuvant RT treatment plans, allowing us to develop a specific predictor of RT response. DNA methylation and RNA-seq data were generated on all RTOG-0539 meningiomas to stratify tumors into their respective Molecular Groups as detailed above. Both DNA methylation and gene expression data were used to build predictive models that could individualize risk of early recurrence after surgery and adjuvant RT. For feature selection in our DNA methylation model, univariable Cox regression analysis for PFS in the RTOG-0539 cohort of meningiomas that received surgery and adjuvant RT (intermediate-risk and high-risk groups from the original trial; $n = 58$ meningioma cases) were computed for all probes covered by the EPIC 850K and v.2.0 array to create a rank list of prognostic, discriminative probes. A total of 1,791 probes that were significantly correlated with PFS after surgery and adjuvant RT at a significance level of $P < 0.001$ were selected to move forward to the subsequent feature selection step. Next, differential methylation analysis was performed between meningiomas from this same RTOG-0539 cohort that progressed/recurred after surgery and adjuvant RT within 3 years of treatment versus those that remained stable within

the same period. This was done to further refine the specificity of DNA methylation probes associated with progressive/recurrent disease cases versus stable disease after surgery and RT. These 15,137 significant (FDR-adjusted $P < 0.05$), highly differentially methylated probes ($\Delta\beta \geq 0.10$ or ≤ -0.10) were then overlapped with probes selected from the univariable analysis (1,791 abovementioned probes), and a set of common probes specific for response to RT were selected as the final features for model building (685 probes). To build the molecular RT model, extreme gradient boosting (XGBoost; xgboost R package (v.1.7.5.1)) modeling was performed using these final 685 probes in the RTOG-0539 training cohort to create and tune a molecular DNA methylation-based predictor of early (3-year) recurrence/progression after surgery and adjuvant RT. A 3-year cutoff was used as this was also the primary outcome of interest in the RTOG-0539 clinical trial. This model was then evaluated on two independent validation cohorts consisting exclusively of meningiomas from the University Health Network (Toronto) that received both surgery and RT ($n = 154$) and a cohort with cases combined from multiple other institutions (Indiana University, Fred Hutchinson Cancer Center, Case Western, Tubingen, Unity Health and Vancouver General Hospital; $n = 122$). Model performance for predicting PFS at 3 years (primary outcome of the RTOG-0539 trial) was assessed by generating receiver operating characteristic (ROC) curves and computing the average AUC and its 95% CI, using bootstrap resampling with 10,000 resamples (pROC R package (v.1.18.4)). The performance of this model was compared with an analogously trained XGBoost model using the 2021 WHO grade alone. There was no overlap between the samples used to train these models and the samples used in the testing/validation cohorts. The 95% CIs for the AUCs of both models were generated using bootstrap resampling with 10,000 resamples for the validation cohorts only. The difference in performance between the two models was compared by computing an average ΔAUC ($\text{AUC}_{\text{Molecular RT Model}} - \text{AUC}_{\text{Clinical Standard of Care Model}}$) and its 95% CI in the same independent validation cohorts. Determination of an optimal cutpoint to dichotomize the validation cohorts into an RT-resistant and an RT-sensitive group was determined using the cutpointR package for a risk score cutoff that maximized the Youden index for predicting PFS after surgery and RT (RT-specific PFS)⁶⁰.

RT gene expression model building

To develop a prognostic set of genes that could predict response to RT, differential gene expression analysis was performed between meningioma cases in the RTOG-0539 cohort with gene expression data that recurred early (≤ 3 years) after surgery and adjuvant RT ($n = 14$ cases) and cases that remained stable after this timepoint ($n = 45$). Differential gene expression was assessed using DESeq2 (v.1.26.0), using negative binomial generalized linear models for each gene⁶¹. Subsequently, Wald's test was applied to obtain P values, followed by Benjamini–Hochberg adjustment for controlling multiple testing. Genes were ranked based on a combined metric incorporating both FC direction and computed P values, computed as $\text{sign}(\log\text{FC}) \times -\log_{10}(P \text{ value})$. Here, the sign of $\log\text{FC}$ indicates the direction of change (positive for upregulation and negative for downregulation), whereas $-\log_{10}(P \text{ value})$ indicates the significance level. Subsequently, Gene Set Enrichment Analysis (GSEA, v.3.0) was conducted as previously detailed, using the ranked scores to discern potential involvement of differentially expressed genes in shared biological pathways. For feature selection of specific genes that may determine response to RT, an FDR cutoff of 0.05 and a $|\log\text{FC}|$ cutoff of 0.57 (representing a 1.5 \times change in expression) were set, above which genes would be considered as significantly prognostic. This produced a predictive set of 26 genes (Extended Data Table 3) that was subsequently passed into a LASSO Cox regression model in our RTOG-0539 training cohort to obtain a set of coefficients for each gene. Risk scores were generated by multiplying the coefficients for each gene by their normalized counts (counts per million (CPM)) and scaled to a value between 0 and 1. In

keeping with previous publications, bootstrap aggregation was then used to train 500 ridge-regression submodels using normalized and log-transformed gene counts as the input variable and risk scores generated in the training cohort as the output to obtain an aggregated risk score for each sample (rms R package (v.6.7-1) and hdnom R package (v.6.0.2))³⁴. These risk scores were then applied to all cases in the retrospective validation cohort ($n = 120$) comprising cases with matched DNA methylation and RNA-seq data, none of which was used to train the model. Model performance was assessed in the same manner as the DNA methylation model and benchmarked against a model built using standard-of-care WHO grade alone.

Combined DNA methylation and RNA-seq model

To develop a model that used both DNA methylation and gene expression data, the risk scores generated by the two respective models above and the same cases in the RTOG-0539 cohort with matched DNA methylation and RNA-seq data ($n = 58$) were used. The probability scores derived from both the XGBoost methylation model and the RNA expression risk score derived from the 26-gene expression model were normalized to a range of 0–1 and served as the exclusive training features for a glmnet model. Logistic regression with the 'binomial' family was employed for model training using the glmnet method. This model was subsequently applied to a matched retrospective validation cohort with corresponding DNA methylation and RNA-seq data for meningioma analysis. Assessment of model performance and discrimination of an optimal cutpoint to dichotomize the validation cohort were completed using the same methodologies as above for each of the individual molecular models.

Clinical and molecular nomogram development

Two distinct elastic net Cox proportional hazards models were developed to forecast PFS after surgery and RT, leveraging methylation data and clinical variables, correspondingly. The choice of the elastic net regularization method aimed to address potential multicollinearity and identify the most informative predictors. Model training was conducted using a training dataset derived from the RTOG cohort. Cross-validation employing three folds facilitated the optimization of model hyperparameters, with the lambda.min rule used to ascertain the optimal penalization parameter. Nomograms were subsequently devised based on the trained models to visually represent the anticipated probability of 3-year PFS after RT for individual patients. These nomograms encompassed the chosen predictors, including methylation probabilities, grade, EOR and RT dose, alongside their corresponding coefficients derived from the Cox models. Predicted probabilities were specifically generated at a time point of 3 years after RT. The predictive efficacy of the methylation-based model underwent evaluation using an external validation dataset. Time-dependent AUC statistics were computed to gauge the discriminatory capacity of the model across varying time intervals. Additionally, the concordance index (C-index) and calibration plots were scrutinized to assess model performance. AUC ROC values were calculated for these models using the same methodology as described above for the DNA methylation and gene expression models, along with their respective 95% CIs, achieved through bootstrap resampling comprising 10,000 resamples.

Statistical analysis

All statistical analyses were carried out using R v.4.2.2 (ref. 12). PFS was compared between groups using a Cox proportional hazards model. Statistical significance was taken to be $P < 0.05$ unless otherwise specified. Survival analyses were performed using Kaplan–Meier methods and fitting Cox proportional hazards models. The proportional hazards assumption was tested by plotting the scaled Schoenfeld residuals of covariates in the model against time and using both individual and global Schoenfeld tests (Supplementary Fig. 1).

does not necessarily reflect the views or policies of the US Department of Health and Human Services nor does mention of trade names, commercial products or organizations imply endorsement by the US Government. Additional funding for this study was provided by the Canadian Institutes of Health Research (CIHR) Project Fund (RN482811-481519; G.Z., F.N. and J.Z.W.), Brain Tumor Charity United Kingdom (GN-000430; GN-000693; G.Z. and F.N.), the UHN Foundation, Mary Hunter Meningioma Research Fund, the V Foundation for Cancer Research (G.Z.), the CIHR Vanier Scholarship (F.N., J.Z.W. and C.G.), the American Association of Neurological Surgeons Neurosurgery Education & Research Foundation Research Fellowship (F.N. and J.Z.W.), the Congress of Neurological Surgeons Tumor Section (F.N. and J.Z.W.) and the Princess Margaret Hospital Foundation Hold 'em For Life Oncology Fellowship (F.N., J.Z.W., A.P.L. and C.G.).

Author contributions

Manuscript writing, figure preparation, general statistical analysis and general bioinformatics were performed by J.Z.W. Molecular classification, model building and bioinformatics support was provided by V.P., A.P.L. and J.L. *TERT* promoter sequencing was performed by C.G. Copy number variant analysis and calling were performed by A.P.L. Molecular analyte extraction, quantification and sequencing were performed by J.Z.W., A.P.L., C.G., A.A. and Z.P. DKFZ methylation class and subclass determination was performed by R.Y. and R.K. using the publicly available online tool created by F.S. RNA sequencing analysis was performed by V.P. and J.L. Biostatistical review was performed by O.S. Clinical data from the NRG Oncology RTOG-0539 meningioma cases were provided by S.L.P. and M.W. Clinical meningioma samples and matching clinical data were

provided by C.W., A.C.G., M.A.Z., G.T., M.T., F.B., D.A.A.B., E.C.H., J.B.S., A.E.S., C.H., S.C., L.B.C., A.R., S.M. and S.Y. Pathologic review was performed by A.G. and K.A. Radiotherapy data of institutional retrospective meningioma cases were provided by D.S.T. Study design and conception were done by J.Z.W, F.N. and G.Z. All authors participated in manuscript review and revisions in some capacity.

Competing interests

S.Y. is a member of advisory boards and has received honoraria from AstraZeneca, Amgen, Bayer, Janssen, Pfizer, Roche and Servier. The remaining authors declare no competing interests.

Additional information

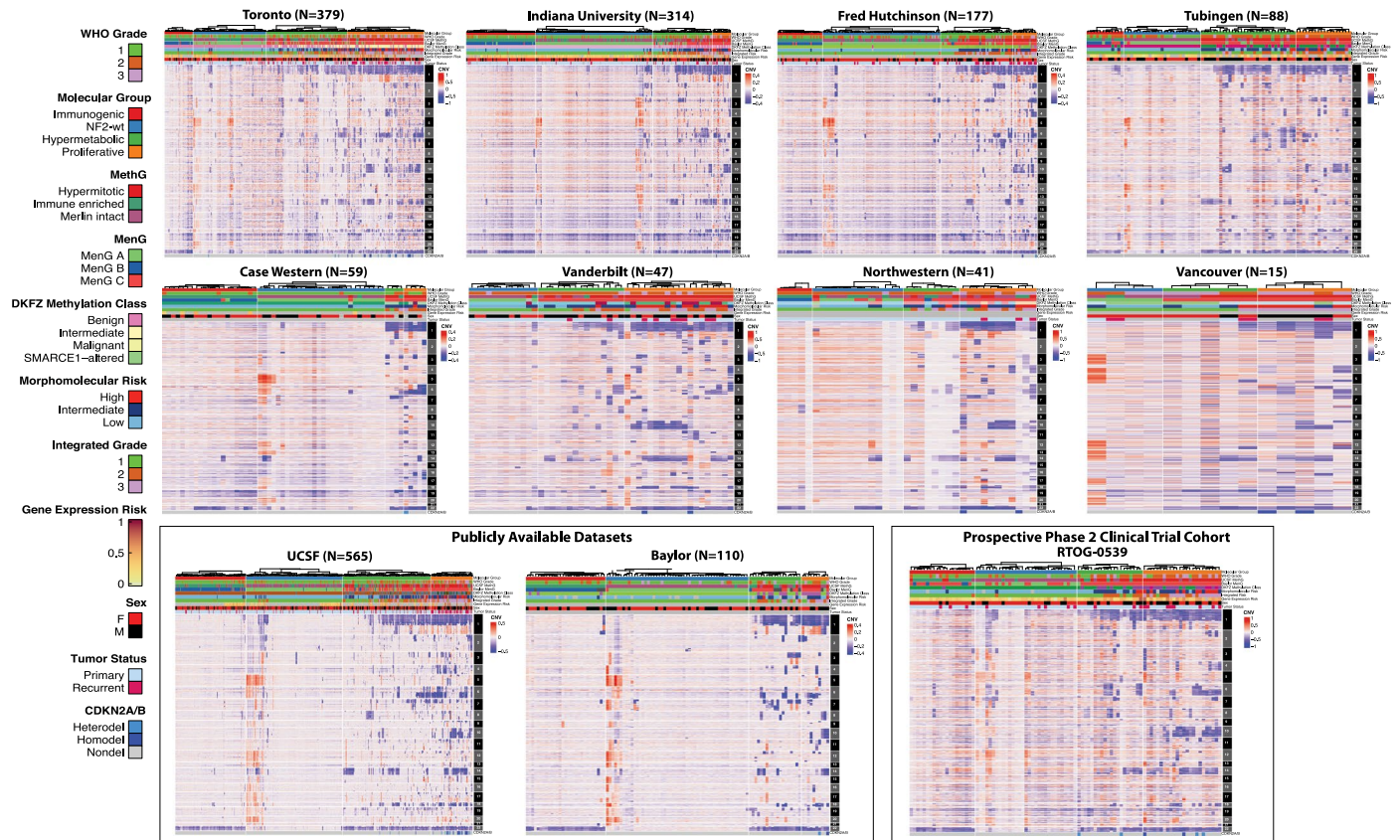
Extended data is available for this paper at <https://doi.org/10.1038/s41591-024-03167-4>.

Supplementary information The online version contains supplementary material available at <https://doi.org/10.1038/s41591-024-03167-4>.

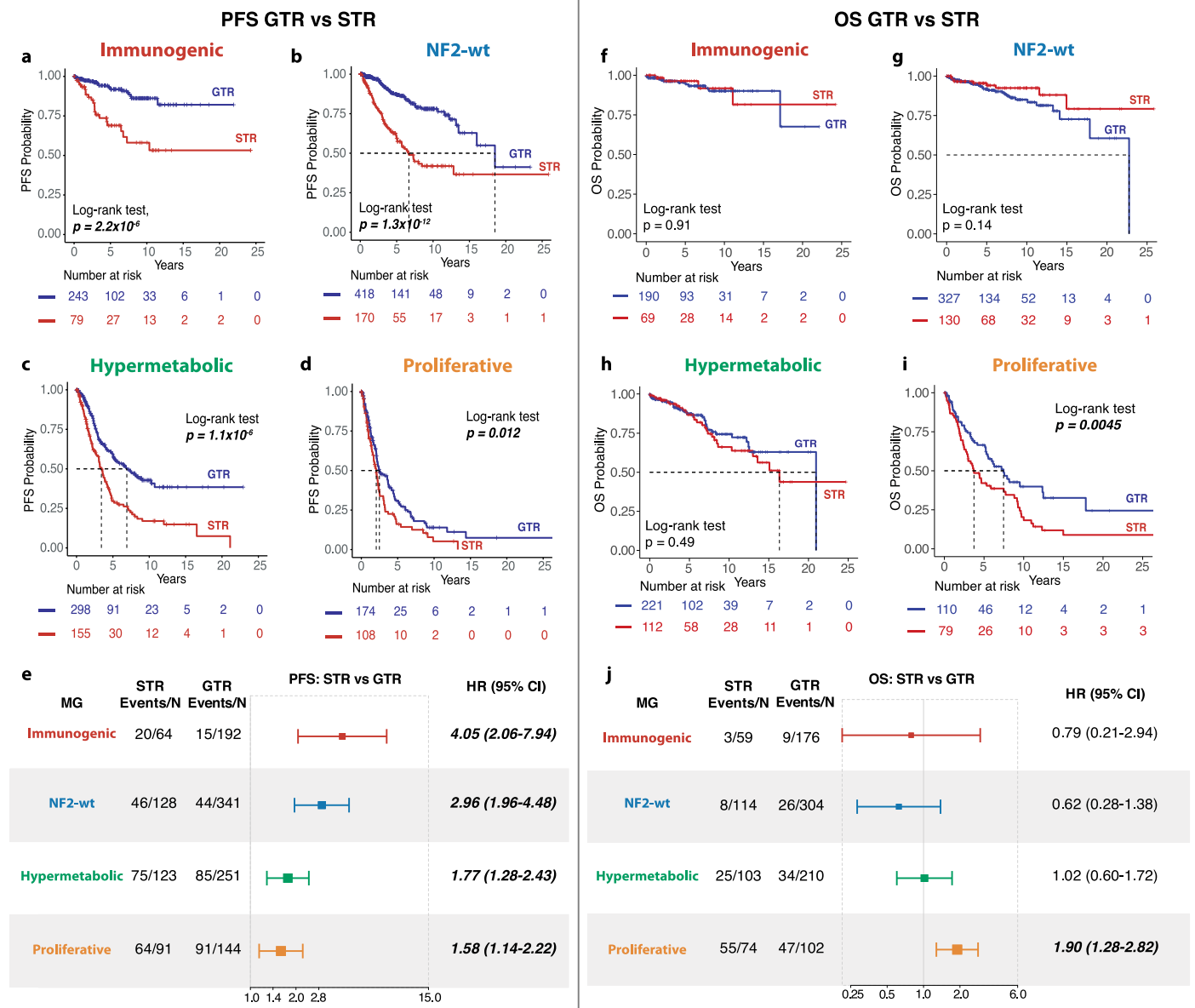
Correspondence and requests for materials should be addressed to Farshad Nassiri or Gelareh Zadeh.

Peer review information *Nature Medicine* thanks Annette Molinaro, E. Antonio Chiocca and the other, anonymous, reviewer(s) for their contribution to the peer review of this work. Primary Handling Editor: Ulrike Harjes, in collaboration with the *Nature Medicine* team.

Reprints and permissions information is available at www.nature.com/reprints.



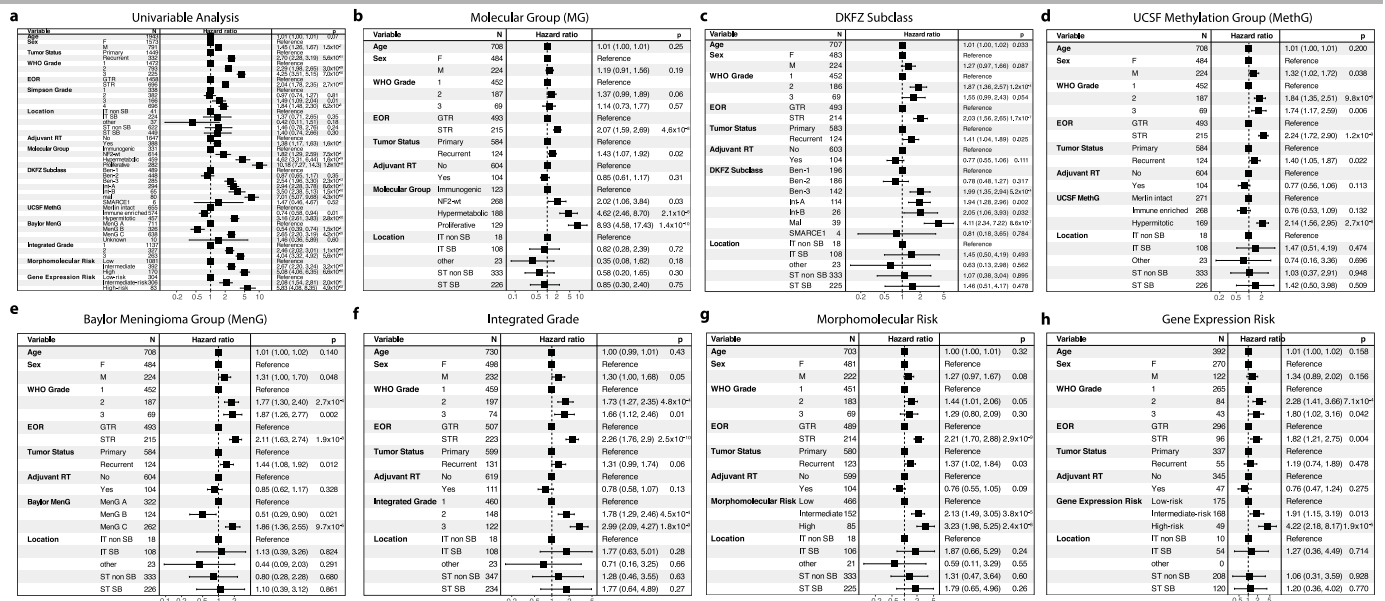
Extended Data Fig. 1 | Copy number variation (CNV) plot in each molecular cohort. CNVs were derived based on inference from DNA methylation data organized based on molecular group (MG) assignment and by institution, including publicly available datasets utilized as well as the prospective RTOG-0539 clinical trial cohort.



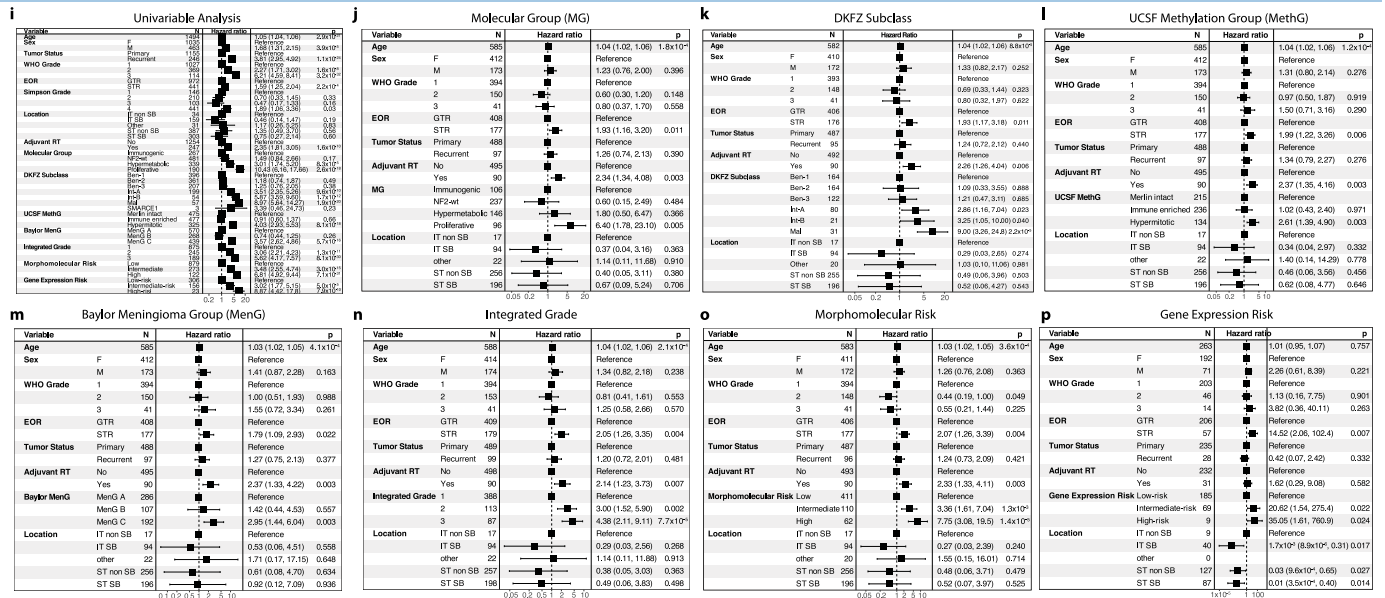
Extended Data Fig. 3 | Benefits of extent of surgical resection (EOR) across Molecular Groups (MG). (a-b) Kaplan-Meier (KM) survival curve showing PFS of meningiomas that received a GTR vs STR belonging to the following MG: Immunogenic (a), NF2-wildtype (b), Hypermetabolic (c), Proliferative (d). e. Results of the multivariable Cox regression analysis assessing the PFS benefits of EOR while controlling for age, sex, WHO grade, primary/recurrent tumor status, and receipt of adjuvant RT with an interaction term between EOR and MG.

(f-i) KM survival curve showing OS of meningiomas based on EOR (GTR vs STR) in each MG: Immunogenic (f), NF2-wildtype (g), Hypermetabolic (h), Proliferative (i). j. Results of multivariable Cox regression analysis on the effect of EOR on OS while controlling for age, sex, WHO grade, primary/recurrent tumor status, and receipt of adjuvant RT with an interaction term between EOR and MG. Box size for the forest plots in (e) and (j) are relative to the weight of the effect size with its center representing the HR and the horizontal error bars representing the 95% CI.

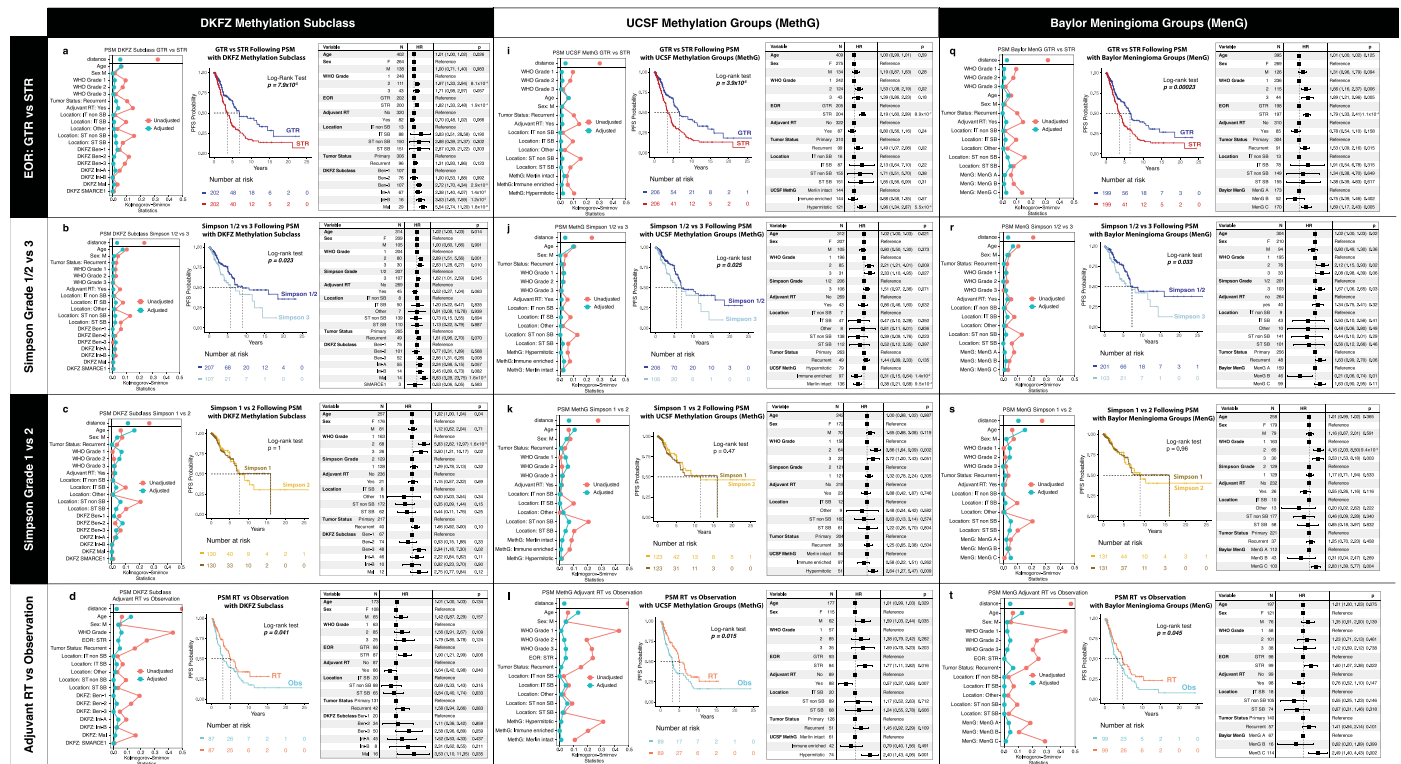
Progression-Free Survival (PFS)



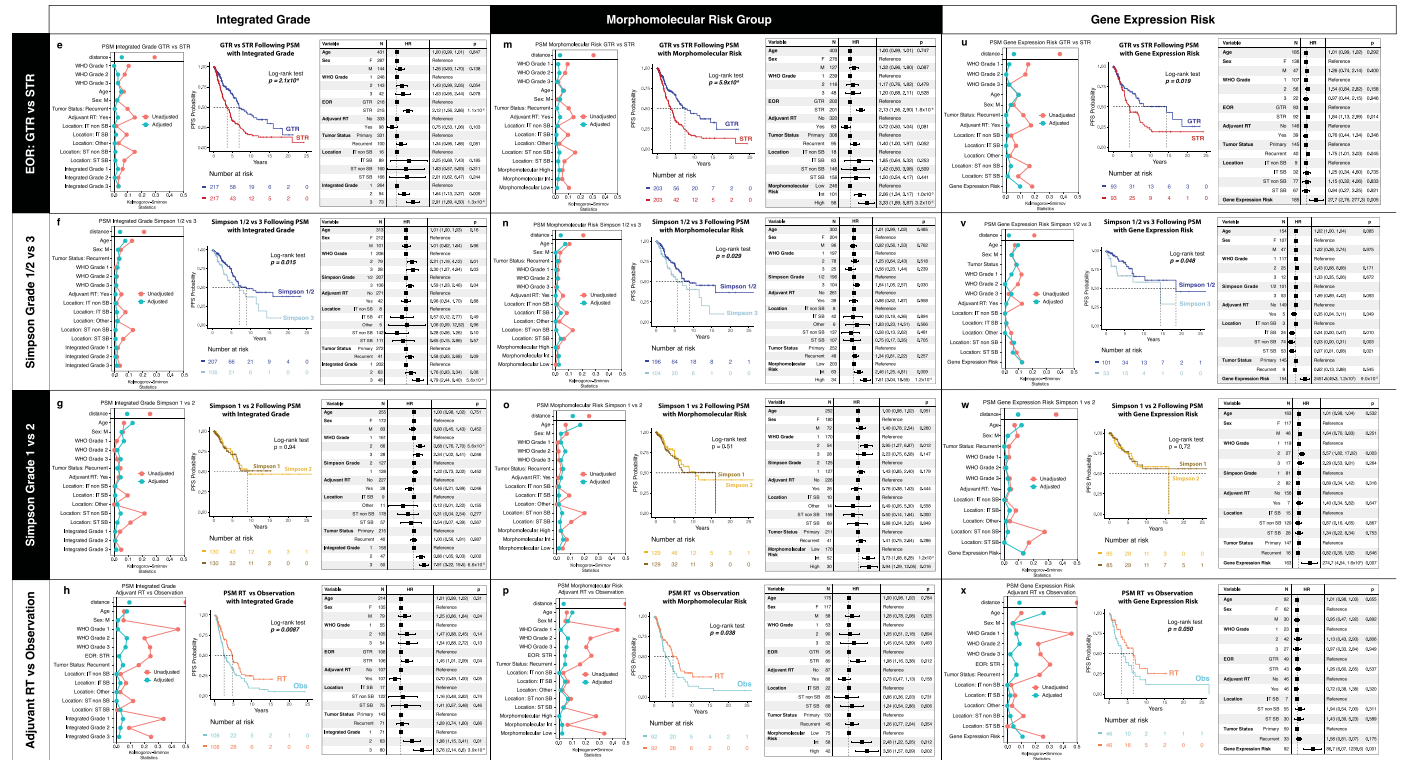
Overall Survival (OS)



Molecular Classification Systems



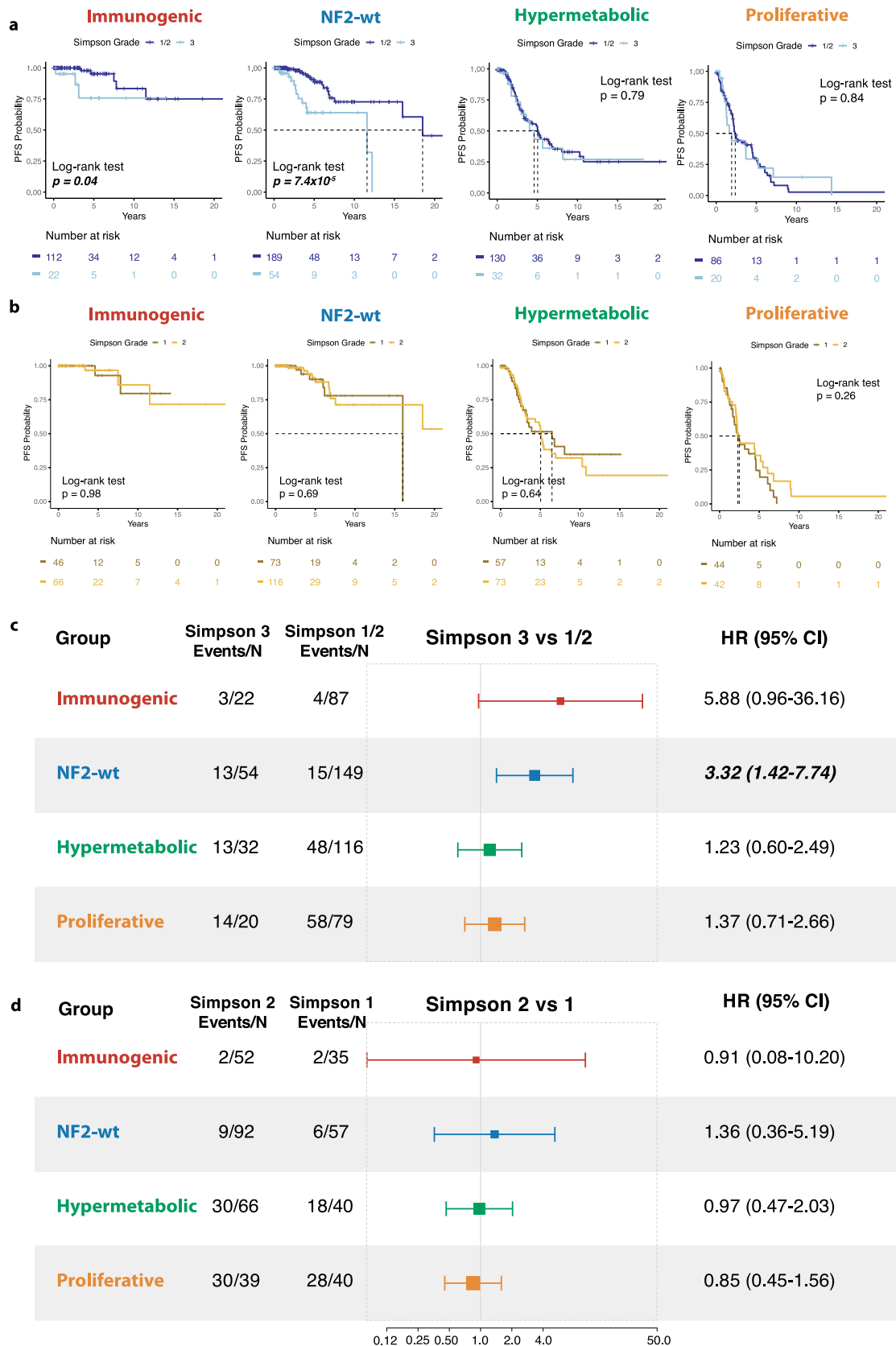
Integrated Molecular Prognostic Systems



Extended Data Fig. 5 | PSM analyses using other molecular classifications and integrated molecular prognostic systems. (a-x) From left to right: love plot, KM survival curve, and results of multivariable Cox regression analyses after PSM for GTR vs STR, Simpson grades 1/2 vs 3, Simpson grade 1 vs 2, and RT vs observation using the DKFZ methylation subclasses (a-d), UCSF MethG (e-h), Baylor MenG (i-t), Integrated Grade (e-h), Morphomolecular Risk (m-p), and

Gene Expression Risk (u-x). Horizontal error bars in the forest plots of represent the 95% confidence interval of the hazard ratios for each of the covariates included in the multivariable Cox regression models presented. P-values for each covariate in the multivariable Cox regression were derived from the Wald test (two-tailed) without adjustments for multiple comparisons.

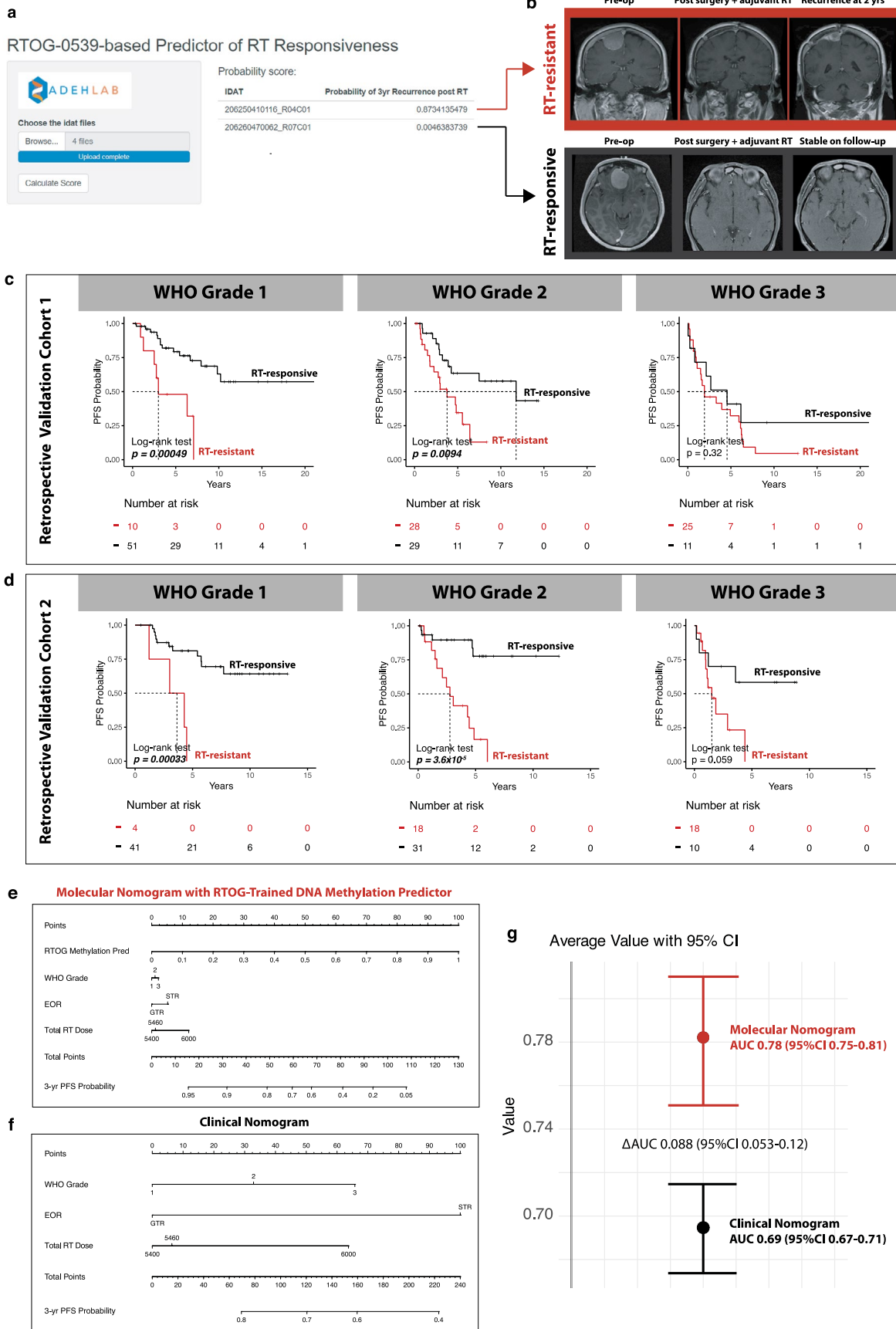
PFS by Simpson Grade



Extended Data Fig. 6 | See next page for caption.

Extended Data Fig. 6 | Prognostic role of Simpson Grade resection across Molecular Groups. **a.** PFS in each Molecular Group (MG) based on grouping meningiomas that received a Simpson grade 1 or 2 resection together vs those that received a Simpson grade 3 resection. **b.** PFS in each Molecular Group for meningiomas that received a Simpson grade 1 resection vs a Simpson grade 2 resection. **(c-d)** Results from the multivariable Cox proportional hazards model showing the effect of Simpson grade on PFS when controlling for age, sex, WHO

grade, receipt of adjuvant RT, and tumor location with an interaction term between Simpson Grade and Molecular Group. Box size for the forest plots in **(c)** is relative to the weight of the effect size with its center representing the HR and horizontal error bars representing the 95% confidence interval of the hazard ratios for each of the covariates included in the multivariable Cox regression models presented.



Extended Data Fig. 7 | See next page for caption.

Extended Data Fig. 7 | RTOG-0539 trained DNA methylation model of RT response and molecular nomogram. **a.** Representative screenshot of DNA methylation .idat files uploaded for 2 separate samples and their respective probabilistic risk of recurrence within 3 years of surgery and adjuvant RT on the publicly available RTOG DNA methylation predictor site. **b.** representative magnetic resonance images of the same sample cases uploaded to the predictor in panel (a) with one RT-resistant case demonstrating recurrence within 3 years of clinical follow-up after gross total resection and adjuvant radiotherapy (above), and a different case in another patient (below) demonstrating interval stability after 3-years following similarly gross total resection and adjuvant RT. **(c-d).** RT-specific PFS outcomes of meningiomas within each WHO grade of the first (c) and second (d) retrospective validation cohorts stratified into an RT-resistant and

RT-responsive group based on the predicted DNA-methylation based RT risk score. P-values generated from Log-rank test. **e.** Molecular nomogram built using the DNA methylation based RT predictor, WHO grade, EOR, and RT dose to predict PFS post-surgery and adjuvant RT using the RTOG-0539 cohort as the training cohort. Each variable in the nomogram is scaled accordingly and values/scores for each variable are assigned points which cumulatively add up to estimate a probabilistic risk of recurrence within 3-years of treatment. **f.** clinical nomogram built using the same variables and training cohort as in (e) except without DNA methylation risk score. **g.** AUC and 95% CI demonstrating the predictive accuracy of the molecular and clinical nomogram respectively validated in the same retrospective cohort of RT-treated meningiomas (N=276).

Extended Data Table 1 | Molecular grouping of meningiomas across WHO grade

	WHO Grade 1 (N=1031)	WHO Grade 2 (N=501)	WHO Grade 3 (N=154)
Immunogenic (MG1)	271 (26%)	58 (12%)	2 (2%)
NF2-wt (MG2)	489 (47%)	108 (22%)	17 (12%)
Hypermetabolic (MG3)	232 (23%)	188 (37%)	39 (26%)
Proliferative (MG4)	39 (3%)	147 (29%)	96 (60%)

Distribution of all molecularly profiled cases in each WHO grade with PFS data across Molecular Group with percentages denoting the proportion of cases within each WHO grade belonging to the specific Molecular Group specified in the leftmost column.

Extended Data Table 2 | RTOG-0539 prospective clinical trial cohort

	Molecular Cohort (N=100)
Baseline characteristic	N (%)
Median age (IQR)	56 (49-64)
Biological Sex	
Male	35 (35%)
Female	65 (65%)
Tumour status (at index surgery)	
Primary	79 (79%)
Recurrent	21 (21%)
Missing	0
WHO Grade	
1	49 (49%)
2	37 (37%)
3	14 (14%)
RTOG-0539 Risk Group	
Group 1 (Low-Risk)	38 (38%)
Group 2/3 (Intermediate-High Risk)	62 (62%)
Extent of Resection (EOR)	
GTR	69 (69%)
STR	16 (16%)
Missing	15 (15%)
Adjuvant RT	
Yes	62 (62%)
No	38 (38%)
Molecular Group (MG)	
1 (Immunogenic)	20 (20%)
2 (NF2-wildtype)	31 (31%)
3 (Hypermetabolic)	20 (20%)
4 (Proliferative)	24 (24%)
Unknown	5 (5%)
Methylation Subclass (DKFZ)	
Benign, subclass 1 (Ben-1)	22 (22%)
Benign, subclass 2 (Ben-2)	22 (22%)
Benign, subclass 3 (Ben-3)	22 (22%)
Intermediate, subclass A (Int-A)	21 (21%)
Intermediate, subclass B (Int-B)	4 (4%)
Malignant (Mal)	4 (4%)
SMARCE1-altered	0
Unknown	5 (5%)

Baseline characteristic and Molecular Group assignment for cases from the RTOG-0539 prospective phase 2 clinical trial with molecular data used for analysis.

Extended Data Table 3 | Predictive 26 gene signature of RT response

gene_symbol	gene_type	baseMean	log2FoldChange	lfcSE	stat	pvalue	padj
NDST4	protein_coding	16.14183	-6.45138	1.491184	-4.32635	1.52E-05	0.025134
EPHA5	protein_coding	62.05374	-6.43953	1.2115	-5.31533	1.06E-07	0.001377
UNC13C	protein_coding	69.20289	-6.09722	1.304019	-4.67572	2.93E-06	0.01032
SLC4A10	protein_coding	64.68162	-5.72638	1.340261	-4.27259	1.93E-05	0.025933
NGF	protein_coding	21.19869	-4.61101	0.758666	-6.07779	1.22E-09	3.43E-05
SCUBE1	protein_coding	704.0126	-4.1601	0.851134	-4.88772	1.02E-06	0.004792
GPM6B	protein_coding	185.2759	-4.02377	0.796786	-5.05	4.42E-07	0.003113
MOXD1	protein_coding	14.42661	-3.1687	0.707015	-4.48179	7.40E-06	0.018966
TNC	protein_coding	504.6852	-3.10182	0.702565	-4.41499	1.01E-05	0.023327
F11	protein_coding	25.66302	-3.07796	0.740062	-4.15906	3.20E-05	0.032168
FSIP2	protein_coding	187.4955	-3.04568	0.699069	-4.35677	1.32E-05	0.023327
MEDAG	protein_coding	202.0542	-2.97035	0.620716	-4.78537	1.71E-06	0.006872
MYLK	protein_coding	1458.376	-2.78112	0.529043	-5.25688	1.47E-07	0.001377
B3GALT1	protein_coding	174.1834	-2.75873	0.671134	-4.11056	3.95E-05	0.037082
FBLN1	protein_coding	944.5201	-2.63582	0.623007	-4.2308	2.33E-05	0.028535
CRISPLD2	protein_coding	296.6113	-2.04908	0.499998	-4.09818	4.16E-05	0.037793
ENPP1	protein_coding	510.0902	-1.91331	0.46766	-4.09124	4.29E-05	0.037793
FUOM	protein_coding	33.18035	-1.83209	0.427233	-4.28828	1.80E-05	0.025933
RNF122	protein_coding	36.73631	-1.79532	0.428426	-4.19049	2.78E-05	0.031381
VAMP5	protein_coding	54.69496	-1.67787	0.402313	-4.17056	3.04E-05	0.031718
SLC16A3	protein_coding	614.2797	-1.46195	0.355111	-4.11688	3.84E-05	0.037082
CSGALNACT1	protein_coding	394.8307	-1.4506	0.336547	-4.31024	1.63E-05	0.025535
SH3TC1	protein_coding	924.2983	-1.40327	0.349822	-4.01139	6.04E-05	0.048608
KLHL6	protein_coding	301.3632	-1.28038	0.313722	-4.08126	4.48E-05	0.038257
ZNF808	protein_coding	773.6995	0.597087	0.122152	4.888056	1.02E-06	0.004792
FLG	protein_coding	29.1003	3.502647	0.863454	4.056552	4.98E-05	0.041285

Highly differentially expressed genes in the RTOG-0539 training cohort used in building the gene expression model of RT response. *P* value and adjusted *P* value were obtained from Wald's test with and without Benjamini–Hochberg correction. lfc, log₂ fold change standard error; stat, Wald's test statistic.

Reporting Summary

Nature Portfolio wishes to improve the reproducibility of the work that we publish. This form provides structure for consistency and transparency in reporting. For further information on Nature Portfolio policies, see our [Editorial Policies](#) and the [Editorial Policy Checklist](#).

Statistics

For all statistical analyses, confirm that the following items are present in the figure legend, table legend, main text, or Methods section.

- | n/a | Confirmed |
|-------------------------------------|--|
| <input type="checkbox"/> | <input checked="" type="checkbox"/> The exact sample size (n) for each experimental group/condition, given as a discrete number and unit of measurement |
| <input type="checkbox"/> | <input checked="" type="checkbox"/> A statement on whether measurements were taken from distinct samples or whether the same sample was measured repeatedly |
| <input type="checkbox"/> | <input checked="" type="checkbox"/> The statistical test(s) used AND whether they are one- or two-sided
<i>Only common tests should be described solely by name; describe more complex techniques in the Methods section.</i> |
| <input type="checkbox"/> | <input checked="" type="checkbox"/> A description of all covariates tested |
| <input type="checkbox"/> | <input checked="" type="checkbox"/> A description of any assumptions or corrections, such as tests of normality and adjustment for multiple comparisons |
| <input type="checkbox"/> | <input checked="" type="checkbox"/> A full description of the statistical parameters including central tendency (e.g. means) or other basic estimates (e.g. regression coefficient) AND variation (e.g. standard deviation) or associated estimates of uncertainty (e.g. confidence intervals) |
| <input type="checkbox"/> | <input checked="" type="checkbox"/> For null hypothesis testing, the test statistic (e.g. F , t , r) with confidence intervals, effect sizes, degrees of freedom and P value noted
<i>Give P values as exact values whenever suitable.</i> |
| <input checked="" type="checkbox"/> | <input type="checkbox"/> For Bayesian analysis, information on the choice of priors and Markov chain Monte Carlo settings |
| <input checked="" type="checkbox"/> | <input type="checkbox"/> For hierarchical and complex designs, identification of the appropriate level for tests and full reporting of outcomes |
| <input type="checkbox"/> | <input checked="" type="checkbox"/> Estimates of effect sizes (e.g. Cohen's d , Pearson's r), indicating how they were calculated |

Our web collection on [statistics for biologists](#) contains articles on many of the points above.

Software and code

Policy information about [availability of computer code](#)

Data collection	Clinical data were collected for patients with meningiomas from 10 different participating institutions of the International Consortium on Meningiomas (ICOM) by expert clinicians including neurosurgeons, neurooncologists, and radiation oncologists specializing in the treatment of meningiomas at their respective institution. Meningiomas were operated on between 2000 to 2020 and enriched for clinical aggressiveness or higher World Health Organization (WHO) grade tumors. Specific data elements collected were in accordance with pre-established common data elements designed for studies on meningiomas and included age, sex, tumor status (recurrent or primary at the time of surgery), WHO grade, Simpson grade, receipt of adjuvant radiotherapy (RT), histological subtype, and location. Meningiomas were graded by experienced neuropathologists from each institution in accordance with either the 2016 or 2021 WHO classification and central pathological review was performed at the University Health Network in Toronto where slides were available. Data from additional publicly available repositories were also collected (GSE189521 (Bayley et al. DNA methylation), GSE183656 (Choudhury et al. DNA methylation and RNAseq)).
Data analysis	The open-source software, tools, and packages used for data analysis in this study, as well as the version of each program, were as follows: ImageJ (v2.1.0), R (v4.3.1), FastQC (v0.11.5), STAR (v2.4.2a), caret R package (v6.0-94), Rtsne R package (v0.16), survival R package (v3.5-5), xgboost R package (v1.7.5.1), glmnet R package (v 4.1-8), rms R package (v6.7-1), hdnom R package (v6.0.2), pROC R package (v1.18.4), minfi (Bioconductor v1.46.0), DESeq2 (Bioconductor v1.26.0), HtSeq R package (v0.11.0), MatchIt R package (v4.5.5), MatchThem R package (v1.1.0), NMF R package (v 0.27). Our DNA methylation model is publicly available and accessible at https://www.meningiomaconsortium.com/models/

For manuscripts utilizing custom algorithms or software that are central to the research but not yet described in published literature, software must be made available to editors and reviewers. We strongly encourage code deposition in a community repository (e.g. GitHub). See the Nature Portfolio [guidelines for submitting code & software](#) for further information.

Data

Policy information about [availability of data](#)

All manuscripts must include a [data availability statement](#). This statement should provide the following information, where applicable:

- Accession codes, unique identifiers, or web links for publicly available datasets
- A description of any restrictions on data availability
- For clinical datasets or third party data, please ensure that the statement adheres to our [policy](#)

DNA methylation data and gene expression data (RNA-sequencing) generated for this study are deposited in the NCBI Gene Expression Omnibus (<https://www.ncbi.nlm.nih.gov/geo/>) under the superseries accession number GSE270375. Unprocessed DNA methylation data from retrospective meningioma tumors are available under the accession number GSE270371 and gene expression counts data are available under the accession number GSE270638. Unprocessed RNA-sequencing data (FASTQ) are deposited in the NCBI Sequencing Reads Archive (<https://www.ncbi.nlm.nih.gov/sra>) under the project number PRJNA1127224 for the retrospective meningioma tumors. Unprocessed DNA methylation data and gene expression data (RNA-sequencing) for the prospective NRG RTOG-0539 clinical trial cases are deposited in the database of Genotypes and Phenotypes (dbGaP) under the project #phs003707.v1.p1 entitled: "MP2PRT-MNG: Identifying novel molecular markers of response to radiotherapy in meningiomas using samples from the RTOG-0539 (NCT00895622)." Previously published, publicly available data were downloaded from the GEO database the GEO database (<https://ncbi.nlm.nih.gov/geo>) under the following accession numbers: GSE189521 (Bayley et al. DNA methylation) and, GSE183656 (Choudhury et al. DNA methylation and RNA sequencing).

Research involving human participants, their data, or biological material

Policy information about studies with [human participants or human data](#). See also policy information about [sex, gender \(identity/presentation\), and sexual orientation](#) and [race, ethnicity and racism](#).

Reporting on sex and gender

Sex data was collected on all patients when available and reported in aggregate. A total of 1793 out of 2824 patients from the retrospective meningioma cohort were female. Of the retrospective cases with molecular data, a total of 1116 out of 1686 patients were female. A total of 65 out of 100 patients from the prospective RTOG-0539 clinical trial cohort were female. Sex and/or gender was not considered in the initial study design given that it has been well established that epidemiologically the majority of meningioma patients are female and that male patients tend to have higher grade, and more biologically aggressive meningiomas. However, this was taken into consideration in data analysis as biological sex was included as a covariate in nearly all univariable and multivariable models and included as a key covariate in propensity score matching.

Reporting on race, ethnicity, or other socially relevant groupings

Ethnicity data was unfortunately not available for the majority of cases utilized in the study and was therefore not integrated into analysis. However, our cohort were comprised of cases from Canada, the United States, and Germany.

Population characteristics

Median age of the total retrospective cohort, the molecular retrospective cohort, and the prospective RTOG-0539 clinical cohort were 57.0, 57.8, and 56.5 respectively. Other relevant demographic data of our cohort are reported in detail in our manuscript and associated tables.

Recruitment

Clinical data were collected for patients with meningiomas from 10 different participating institutions of the International Consortium on Meningiomas (ICOM) and using publicly available data repositories by expert clinicians including neurosurgeons, neurooncologists, and radiation oncologists specializing in the treatment of meningiomas at their respective institution. Cases were operated on between 2000 to 2020 and enriched for clinical aggressiveness or higher WHO grade tumors. Specific data elements collected were in accordance with pre-established common data elements designed for studies on meningiomas and included age, sex, tumor status (recurrent or primary at the time of surgery), WHO grade, Simpson grade, receipt of adjuvant radiotherapy (RT), histological subtype, and location. Meningiomas were graded by experienced neuropathologists from each institution in accordance with the 2021 WHO classification and central pathological review was performed at the University Health Network in Toronto for cases where slides were available. Data collection of these cases are nonetheless still subject to the inherent biases of retrospective data collection which includes selection biases associated with the majority of cases originating from tertiary academic neurosurgical centres. The RTOG-0539 (NCT00895622) is a prospective, phase 2, non-randomized clinical trial that stratified patients with meningiomas to adjuvant RT (or observation) treatment arms based on WHO grade, EOR, and primary/recurrent tumor status. Tissue for molecular profiling and clinical data from the RTOG-0539 trial were obtained through The Molecular Profiling to Predict Response to Treatment (MP2PRT) program as part of the National Cancer Institute's Cancer Moonshot Initiative.

Ethics oversight

Ethics approval for this study was provided by the Research Ethics Board via the Coordinated Approval Process for Clinical Research at the University Health Network (Toronto, ON) locally under CAPCR 18-5820 and by relevant institutional review board (IRB) at all included institutions (Indiana University, Case Western Reserve University, University of Tubingen, Vanderbilt University, Vancouver General Hospital, Fred Hutchinson Cancer Center, Northwestern University)

Note that full information on the approval of the study protocol must also be provided in the manuscript.

Field-specific reporting

Please select the one below that is the best fit for your research. If you are not sure, read the appropriate sections before making your selection.

- Life sciences Behavioural & social sciences Ecological, evolutionary & environmental sciences

For a reference copy of the document with all sections, see [nature.com/documents/nr-reporting-summary-flat.pdf](https://www.nature.com/documents/nr-reporting-summary-flat.pdf)

Life sciences study design

All studies must disclose on these points even when the disclosure is negative.

Sample size	No sample size calculation was used. All retrospective samples included represented all available meningioma datasets from each respective institution with accompanying tissue for molecular profiling, previously published molecular data, or clinical data only. Sample size calculation for the completed RTOG-0539 prospective clinical trial were as per protocol of the original trial with 100 cases having sufficient tissue for molecular profiling. This dataset represents that largest molecular meningioma dataset with detailed clinical data on extent of surgical resection, adjuvant radiotherapy, and clinical follow-up.
Data exclusions	Data were excluded for cases that failed QC on DNA methylation or RNA-seq. We also excluded meningiomas from molecular classification when their DNA methylation profile did not classify reliably as meningioma on the DKFZ methylation classifier or did not cluster with meningiomas on a t-distributed Stochastic Neighbor Embedding with other confirmed reference meningioma cases, thereby ensuring our cohort was comprised entirely of molecularly-confirmed meningiomas for analysis. Otherwise, all patients with available molecular data and tissue for DNA methylation and/or RNA-seq were included.
Replication	All analyses, including propensity score matching were repeated using 4 different molecular classifications (Toronto molecular group, DKFZ methylation class/subclass, UCSF Methylation Group, Baylor Meningioma Group), 3 molecular prognostic systems (Integrated Grade, Morphomolecular Risk, Gene Expression Risk) in addition to WHO grade with concordant results across all attempts at replication. To ensure reproducibility, confirmation of molecular group classification for each case were performed by two separate individuals (APL, VP) blinded to clinical outcome using multiple orthogonal approaches including the originally published methodologies as well as utilization of different data types for the same tumor when matched DNA-methylation and RNA-seq were available (see Supplementary Methods in the Extended Data).
Randomization	NA. Randomization was not performed in this study. Univariable and multivariable Cox regression analysis as well as propensity score matching were used to control clinical covariates between treatment arms for this study.
Blinding	All initial molecular classifications and bioinformatic analyses pertaining to molecular classification including in the RTOG-0539 clinical trial were performed by individuals blinded to clinical outcome, institution, and other clinical data (including WHO grade) to ensure unbiased, biologically rooted group allocation independent of outcome.

Reporting for specific materials, systems and methods

We require information from authors about some types of materials, experimental systems and methods used in many studies. Here, indicate whether each material, system or method listed is relevant to your study. If you are not sure if a list item applies to your research, read the appropriate section before selecting a response.

Materials & experimental systems

n/a	Involved in the study
<input checked="" type="checkbox"/>	<input type="checkbox"/> Antibodies
<input checked="" type="checkbox"/>	<input type="checkbox"/> Eukaryotic cell lines
<input checked="" type="checkbox"/>	<input type="checkbox"/> Palaeontology and archaeology
<input checked="" type="checkbox"/>	<input type="checkbox"/> Animals and other organisms
<input type="checkbox"/>	<input checked="" type="checkbox"/> Clinical data
<input checked="" type="checkbox"/>	<input type="checkbox"/> Dual use research of concern
<input checked="" type="checkbox"/>	<input type="checkbox"/> Plants

Methods

n/a	Involved in the study
<input checked="" type="checkbox"/>	<input type="checkbox"/> ChIP-seq
<input checked="" type="checkbox"/>	<input type="checkbox"/> Flow cytometry
<input checked="" type="checkbox"/>	<input type="checkbox"/> MRI-based neuroimaging

Clinical data

Policy information about [clinical studies](#)

All manuscripts should comply with the ICMJE [guidelines for publication of clinical research](#) and a completed [CONSORT checklist](#) must be included with all submissions.

Clinical trial registration	Clinical trial samples used in the study from the NRG Oncology RTOG-0539 study were originally accessed from NCT00895622
Study protocol	Full protocol for the RTOG-0539 clinical trial can be found at https://www.nrgoncology.org/Clinical-Trials/Protocol/rtog-0539?
Data collection	Recruitment, data collection, and locales of data collection have been previously published and documented as part of the NRG Oncology RTOG-0539 clinical studies (PMID 31786276, 28984517, 35657335)
Outcomes	Outcomes from the NRG Oncology RTOG-0539 clinical trial (NCT00895622) were pre-defined and these outcome data were utilized for our study.

Plants

Seed stocks

NA

Novel plant genotypes

NA

Authentication

NA